AMRL-TDR-62-140 (II)

RESEARCH ON SOUND PROPAGATION IN SOUND-ABSORBENT DUCTS WITH SUPERIMPOSED AIR STREAMS

VOLUME II

TECHNICAL DOCUMENTARY REPORT NO. AMRL-TDR-62-140 (II)

December 1962

Biomedical Laboratory
6570th Aerospace Medical Research Laboratories
Aerospace Medical Division
Air Force Systems Command
Wright-Patterson Air Force Base, Ohio

Contract Monitor: William C. Elrod, Captain, USAF
Project No. 7231, Task No. 723104

[Prepared under Contract No. AF 61(052)-112
by
F. Mechel
W. Schilz
III. Physikalisches Institut der Universität Göttingen
Göttingen, Germany]

NOTICES

When US Government drawings, specifications, or other data are used for any purpose other than a definitely related government procurement operation, the government thereby incurs no responsibility nor any obligation whatsoever; and the fact that the government may have formulated, furnished, or in any way supplied the said drawings, specifications, or other data is not to be regarded by implication or otherwise, as in any manner licensing the holder or any other person or corporation, or conveying any rights or permission to manufacture, use, or sell any patented invention that may in any way be related thereto.

Qualified requesters may obtain copies from ASTIA. Orders will be expedited if placed through the librarian or other person designated to request documents from ASTIA.

Do not return this copy. Retain or destroy.

Stock quantities available at Office of Technical Services, Department of Commerce, $2.25.

19-442, 900, 2-18-63

FOREWORD

This report is Volume II of a series of reports on sound propagation in sound absorbent ducts with a superimposed air stream prepared by Göttingen University, Göttingen, Germany, for the Bioacoustics Branch, 6570th Aerospace Medical Research Laboratories, Aerospace Medical Division, under Contract AF 61(052)-112. The work was performed under Project 7231, "Biomechanics of Aerospace Operations," Task 723104, "Biodynamic Environments of Aerospace Flight Operations." Principal Investigators for Göttingen University were Dr. Erwin Meyer and Dr. Fridolin Mechel. Technical and administrative personnel monitoring this effort have included Dr. H. von Gierke, Capt. W. Elrod, R. G. Powell, and J. N. Cole.

Initial research on this investigation commenced in June 1958.

ABSTRACT

This report, Volume II, shows that the attenuation of sound in absorbing ducts with superimposed flow is dependent in a high degree on the direction of the flow and its velocity. The change of attenuation is caused by a convective variation of the acoustic wavelength, by a nonlinear variation of the characteristic constants of the absorber, and by a deformation of the wave fronts in the profile of the mean flow. These changes can be calculated and are in good agreement with the experimental results. In a duct coated with undamped Helmholtz resonators the mechanism of sound amplification is based on the interaction between the sound wave and the turbulence. The conversion of kinetic flow energy into acoustic energy is performed by synchronization of turbulence. For appropriate values for flow velocity and signal frequency a long-range stable wave of pseudo-sound takes place. Sound and pseudo-sound interact with one another at the necks of the resonators.

PUBLICATION REVIEW

This technical documentary report has been reviewed and is approved.

JOS. M. QUASHNOCK
Colonel, USAF, MC
Chief, Biomedical Laboratory

Contents

List of Figures

List of Figures

Part A
List of Symbols

A	absorption coefficient or amplitudes
A_f	frequency dependent parameter
c	adiabatic sound velocity
E	acoustic energy
f	frequency
h	height of duct
k	profile exponent, or total number
K	coupling coefficient.
L	distance between adjacent resonators
M = V/c	Mach number
N	acoustic power
n	total number
r	flow resistance of absorber
R	gas constant
Re	Reynolds number
T	absolute temperature
u	phase velocity
v	alternating or local mean velocities
V	mean flow velocity
x	coordinate in direction of duct axis
y	coordinate perpendicular to duct wall
Z	wall impedance
α	attenuation
γ	angle between wave front and flow
ε	density ratio
η	loss factor

$\varkappa$	adiabatic exponent
$\omega = 2\pi f$	
ρ	density of air
φ	phase angle
σ	porosity of the absorber
ψ	glancing angle of the wave front and phase angle
$\sim$	proportional
$\simeq$	approximately equal

Part B

e	acoustic energy density
f	frequency
G	absorber admittance
k_l	wavenumber in the direction of the duct axis
k_t	transversal wave number
N	acoustic power through the duct
S	cross sectional area of the duct
u_e	energy propagation velocity
u_{gr}	group velocity
u_{ph}	phase velocity
V	flow velocity
α	attenuation constant
α'	attenuation per wavelength
$\alpha^* = \alpha' \frac{1+V/u_{gr}}{1+V/u_{ph}}$	
δ^*	displacement thickness of boundary layer
λ	wavelength
o	as index: for air at rest
V	as index: for superimposed flow with velocity V

Part A

Experiment about the Interaction between Flow and Sound Field in a Wind Tunnel Covered with Porous Absorbers and Helmholtz-Resonators.

SUMMARY

The attenuation of sound in absorbing ducts with superimposed flow is dependent in a high degree on the direction of the flow and its velocity. The change of attenuation is caused by a convective variation of the acoustic wavelength, by a nonlinear variation of the characteristic constants of the absorber and by a deformation of the wave fronts in the profile of the mean flow. These changes can be calculated in good agreement with the experimental results.

In a duct coated with undamped Helmholtz-resonators the mechanism of sound amplification is based on the interaction between the sound wave and the turbulence. The conversion of kinetic flow energy into acoustic energy is performed by synchronization of turbulence. For appropriate values for flow velocity and signal frequency a long range stable wave of pseudo-sound takes place. Sound and pseudo-sound interact with one another at the necks of the resonators.

Introduction

In the past years investigations were performed by F.Mechel [1] at the III.Physikalisches Institut der Universität Göttingen about the influence of flow on the attenuation of air-borne sound in absorbing ducts. The scope of those measurements was to determine the influence of flow on the frequency-response of the attenuation for various types of absorbers. Especially porous absorbers (rockwool) and Helmholtz-resonators were tested. With porous absorbers a strong variation was found for increasing flow velocity and a striking inequality was detected for downstream or upstream propagation respectively. Fig.1 shows the change of attenuation per wavelength in the duct with porous absorbers, where the variation of the wavelength by the flow was taken into account. Positive values of the flow velocity V stand for downstream propagation, negative values mean upstream propagation.

If the duct is covered with Helmholtz-resonators, there is above resonance, which is marked by a high attenuation, a frequency range, where the acoustic input signal is amplified. Flow velocity V_a and frequency f_a of maximum amplification are connected with one another by

$$V_a = \frac{u_o}{2} \left(-1 + \sqrt{1 + \frac{4L}{u_o n} f_a}\right) \quad ,$$

where u_o is the phase velocity of the signal as measured in air at rest, L is the distance between adjacent resonators and n is a integer number, preferably +1. Frequency responses of attenuation and amplification for various flow velocities are plotted in Fig.2.

The scope of this paper is to light up the causes of the change of attenuation with porous absorbers by detailed measurements of the sound field as well as of the distributions of turbulence and mean flow within the duct. Also by anemometric techniques the mechanism of the signal amplification with reactive absorbers will be studied.

§ 1. Kundt's Tube Measurements.

I. Porous Absorbers.

Of the various possible effects of flow on the attenuation in the duct the convective one, meaning the variation of the wavelength in the duct by the superposition of the flow and thereby the variation of the acoustic density in the duct, may be eliminated by calculating the attenuation per wavelength as in Fig.1. The next effect to be explored is the influence of the turbulence on the impedance of the rockwool. This effect becomes important because of the high turbulence level in the duct. The turbulence level in the center of the duct is about 5%, the transversal and longitudinal components of the turbulence increase however strongly towards the walls of the duct. At the absorbers surface the transversal component of the turbulence penetrates into the absorber. Since the flow resistance of porous absorbers - being a quantity, which determines their impedance - is linear only for small velocity amplitudes, it will be modulated into the nonlinear range by the great alternating amplitudes of the turbulent velocities. Because of this nonlinearity a superimposed alternating velocity of an acoustic signal, even if small, will be under the influence of an increased flow resistance. The level of the turbulent velocities is a function of the mean flow velocity. Therefore the absorbers flow resistance r may be expressed as a function of the mean flow velocity V in terms of

$$r = r_o + r(V) \ . \tag{1}$$

For an increasing flow resistance of the absorber the attenuation in the duct decreases, since the absorber becomes more and more mismatched. For a duct with cross dimensions small compared to the wavelength the following approximate proportionality between attenuation α and flow resistance is derived

$$\alpha \sim [r_o + r(V)]^{-1/4} \tag{2}$$

by using the approximation for the wall impedance

$$|z| \approx c_o\sqrt{\frac{\rho}{\omega}}\sqrt{r_o + r(V)} \; . \qquad (3)$$

These approximations are valid for the duct used in the measurements.

The set-up shown in Fig.3 was used to measure the impedance of a porous absorber in presence of a d.c. flow along its surface. The Kundt's tube was terminated by a chamber containing layers of rockwool. The air current enters and emerges through thin borings in opposit walls. The conical mouthpieces guarantee by their strong damping a sufficient acoustical decoupling of the measuring chamber from the air inlets.

As an example of the measurements in Fig.4 is represented the impedance of the absorber in the complex plane. The resonance loop, as determined by the dimensions of the chamber, shrinks with increasing velocity of the d.c. flow. This indicates an increase of the flow resistance of the rockwool and an associated increase of the damping of the chamber. The resonance frequency remains nearly the same. The change of the flow resistance as derived from these measurements is shown in Fig.5, curve A. If very thin layers of rockwool (about 1 mm) are used, this results in a stronger variation of the flow resistance, since now the penetration of the d.c. flow into the rockwool becomes greater (curve B). The imaginary part of the impedance varies only in a small degree as indicated by the constancy of the resonant frequency of the chamber. Therefore the variation of the absorbers impedance measured later on in the duct will be ascribed only to the variation of the flow resistance.

II. Damped Helmholtz-resonators.

By the same method just described also the influence of flow along a damped Helmholtz-resonator on its impedance was measured. The neck of the resonator was covered with a 0.1 mm rockwool sheet, over which the air was blown. In order to

avoid disturbances from the air horns, these were formed as short-circuit members. By these means rigid terminations could be transformed for each frequency into the entrance planes of the air horns into the Kundt's tube. The damping of the resonator, determined from the half widths of the resonance curves increased with increasing flow velocity in a similar manner as with the porous absorber. There was no sensible shift of the resonance frequency. This cannot be expected for the small flow velocities used in the measurements (5 m/sec).

The influences of flow changing the duct attenuation are very much similar for both porous absorbers and strongly damped Helmholtz-resonators. As a consequence the attenuation measurements performed by F.Mechel [1] yield the same dependence on the flow for both types of absorbers.

§ 2. Sound Attenuation in a Duct Covered with a Porous Absorber.

The duct used for the following measurements was of a length of 2.50 m and a free cross-section of 35 mm times 100 mm. The maximum flow velocity was about 80 m/sec. The flow was generated by a one-stage centrifugal blower and was silenced by two mufflers of a total length of 4 m. By these means the flow had a low noise level at the entrance into the measuring duct. The superimposed acoustical signal was generated by two loudspeakers of 200 Watts each. The resulting signal-to-noise ratio was greater than 40 dB.

I. Interrelation between the Change of Impedance and of Attenuation.

The turbulence-induced change of the impedance of a porous absorber, discussed in section II/1, cannot be measured by the method described there for the high flow velocities used in the duct. Therefore an indirect method was developed for the measurement of the flow resistance, which prooved to be the significant term, and its dependence on the velocity of a

turbulent flow along the surface of the absorber. With this method the attenuation of the signal was measured during its propagation through the porous material, which was exposed to the flow. Using the well-known relation between attenuation in and flow resistance of a porous material the dependence of the flow resistance on the flow velocity could be determined. With the equations (2) and (3) the dependence of duct attenuation on flow velocity due to nonlinearity of the flow resistance could be calculated.

Fig.6 shows a sketch of the experimental set-up. A section of the absorber was shielded by a brass tube of about 5 cm diameter from waves propagating in the material. By a pressure probe of 3 mm diameter the pressure drop of the signal wave was measured, as it propagates from the surface A into the absorber.

Without a signal present also the alternating pressure generated by the turbulence could be registered in the same manner. Within the absorber sound and turbulence behave alike. The same attenuation was measured for both of them. The attenuation increases strongly with increasing flow velocity in the duct especially on the side A of the absorber. Since the turbulence amplitude decreases with increasing distance from the surface A, the modulation of the flow resistance and therewith the sound attenuation in the absorber decrease also. Fig.7 shows an example for this dependence from depth.

The approximative calculation of the duct attenuation, equations (2) and (3), assumes a homogeneous absorber. By the flow-induced local variation of the flow resistance in the direction perpendicular to the absorber surface the material becomes inhomogeneous with flow present. Taking into account the measured variations yield a change in the resulting wall impedance of the absorber of about 4%. This change will be compensated in the further evaluations.

By the outlined method the relative change r/r_o of the flow resistance was determined for the frequencies 0.4, 0.6, 1.0, and 1.4 kc respectively. The dependence on the flow velocity is different for all frequencies, but it may be

represented by the common equation

$$r/r_o = (1 - A_f V)^{-4} \quad , \tag{4}$$

where A_f is an empirical, frequency-dependent parameter. This equation and the measured values are represented in Fig.8, where the abscissa is $A_f V$, by which mean all the curves fall together into one. The empirical values of A_f are

$$A_{0,4} = 8 \cdot 10^{-3} \qquad A_{1,0} = 2{,}5 \cdot 10^{-3}$$
$$A_{0,6} = 3{,}5 \cdot 10^{-3} \qquad A_{1,4} = 2{,}3 \cdot 10^{-3}$$

The values of r/r_o do not exceed 3.5. The deviation of the measurements for 0.4 kc, for which frequency the constant A_f differs strongly from the values for other frequencies, must be interpreted therefore by a saturation effect. Because of the smooth course of A_f as a function of frequency, the value of this constant may be easily interpolated for other frequencies than the indicated ones and therefore the change of flow resistance with flow velocity is known for all frequencies.

Combining the equations (2), (3), and (4) the change of the duct attenuation α caused by nonlinearity of the absorber is reduced to the determination of the proper A_f by virtue of the following proportionality

$$\alpha \sim r_o^{-1/4} (1 - A_f V) \tag{5}$$

as long as only the real part of the wall impedance is changed by the change of the flow resistance and as the height of the duct is small compared to the wavelength.

For this correction of the duct attenuation due to the nonlinearity of the absorber the relative direction of signal and flow is obviously of no importance. Using the positive or negative value of V for distinction of downstream or upstream propagation of the signal respectively V in equ.(5) must be replaced by $|V|$. The variation of the duct attenuation due to nonlinearity is plotted in Fig.9 as a function of flow velocity

for various frequencies. The measured values of α represented in Fig.1 are corrected according to Fig.9 and then represented in Fig.10.

After the convective variation of the wavelength in the duct and the nonlinearity of the absorber have been taken into account, the curves for the so corrected attenuation reveal further dependence on the flow velocity and especially a dependence on the relative direction of signal and flow. For downstream propagation the corrected attenuation is independent of flow velocity within the accuracy of measurement, for upstream propagation however the attenuation increases strongly with increasing values of the flow velocity. This behaviour shall be explained in the following sections by the interference between wavefronts of the signal and profiles of the mean flow in the duct.

II. Flow Distribution and Wave Fronts in the Duct.

In order to check the influence of the flow profile, this one must be well known. A hot-wire anemometer with small interference with the flow because of its small size served as a probe for measuring flow distributions and turbulence. Alternating velocities can be registered correctly with respect to amplitude and phase within 2 and 100 000 cycles. The probe can be calibrated for reading absolute values.

By the different structure of the walls of the duct - the upper wall consisted of rockwool, the lower one of polished wood - the flow profile is nonsymmetric with respect to the axis of the duct.

A simple criterion for judgement of the flow profile is available by the universal law for flow in ducts [2]

$$\left(\frac{v}{V}\right)^k = \left(\frac{y}{h}\right) \qquad (6)$$

v = local velocity y = wall distance
V = center velocity $2h$ = height of duct.

By plotting the flow profile in a double-logarithmic scale the exponent k of the profile is determined. The values of k

obtained in this manner are within the range of flows over smooth surfaces. This was to be expected, since the scale of roughness for rockwool is small compared to the boundary layer thickness of 3 to 4 mm. The measured values of k are different from one another for absorber and wood panel. Whereas the values measured at the wooden wall coincide with the theoretical values for corresponding Reynolds number (referring to the height of the duct), the profiles at the absorber surface reveal strong deviations:

V (m/sec)	Re	$K_{meas.}$	$K_{theor.}$
11	$7.3 \cdot 10^4$	5.26	6.8
45	$3.0 \cdot 10^5$	6.67	7.7
55	$3.6 \cdot 10^5$	7.41	7.8

The measured k-values are always smaller than the theoretical ones. An obvious explanation is, that the turbulence of the flow is reduced by the absorber. As the transversal component of the turbulence penetrates into the absorber and is damped there in quite the same manner as the acoustic oscillations, energy of turbulence can be withdrawn in this way.

With the help of the flow profiles now high-frequency-approximations for the phase profiles can be constructed by simple addition of sound velocity and local flow velocity. The term high-frequency-approximation here means, that the sum of the two velocities will represent the true local sound velocity only, if the cross dimensions of the duct and of the flow profile are large compared to the wavelength. This is not true in our case. Nevertheless phase profiles will be constructed in this way for comparison with the phase profiles measured later on.

A sound wave propagating in a moving medium (local velocity v) in (or opposite to) the direction of the flow has a local phase velocity

$$u = u_o \pm v \quad , \qquad (7)$$

where u_o is the phase velocity in air at rest. For qualitative applications v may often be replaced by the flow velocity V_m of the maximum of the flow profile. The profiles of the phase velocity according to equ.(7) are plotted in Fig.12. The upper abscissa is valid for downstream propagation, the lower for upstream propagation. These profiles of the phase velocity determine the deformation of the wave fronts, once an initial form of the wavefront is given.

In a duct with rigid walls the phase surfaces are perpendicular to the walls for air at rest. With absorbent coatings the wavefront is curved already with air at rest in such a way, that the phase at the absorber surface has a certain angle of lag. This curvature results from an interference between the acoustic wave in the duct and acoustic surface waves along the surface of the absorber. The glancing angle between wavefront and absorber is connected to the characteristic values of the absorber by the equation [3]

$$\tan\psi = \frac{1}{\sigma}\sqrt{\frac{2\varepsilon}{\eta}}\;\frac{\eta^2+1}{\eta+1} \qquad (9)$$

σ porosity $\qquad \varepsilon = \rho/\rho_o$ ratio of densities of air inward and outward the absorber

$\eta = \frac{r}{\omega_o}$ loss factor

For air at rest a decrease in ψ indicates greater attenuation.

The initial phase profile at the entrance of the duct is assumed to be given by this relation. During propagation in the air stream the form of the wavefront will be changed continously by virtue of the differences in the local phase velocities. The positions of equal phase after a transition angle $\varphi = 2\pi\frac{x_o u_m}{f}$ are given by the equation

$$x(\varphi,y) = [\varphi - \varphi_o(y)][n_o+v(y,V_m)]\;\omega^{-1} \qquad (10)$$

where $u_m = u_o + V_m$. This equation is evaluated in Fig.13 for $\omega = 2\pi \cdot 600$ cycles and $V_m = 45$ m/sec and different distances x_o traversed. For downstream propagation the wave fronts assume more and more the form of the flow profile. The glancing angle

at the absorber changes only little, however. Significantly greater is the influence of the flow profile for upstream propagation. Here the curvature of the phase profile may be canceled after a short distance traversed. After a way of about 20 cm the direction of the curvature of the phase profile has changed its sign. The zones near the wall show a phase advance. This striking difference for the two directions of propagation is in agreement with Fig.10, where only for upstream propagation the attenuation is dependent on flow velocity.

III. Measurement of the Phase Profiles.

As mentioned already the condition of small wavelength compared to the flow profile thickness is not fulfilled in the present experiments. Therefore the wavefronts were measured directly. As a typical frequency of the signal 600 cycles were used. For this frequency the wavelength is very much greater than the cross dimensions of the duct and the signal-to-noise ratio is sufficient for safe operation of the phasemeter. The situation for other frequencies may be depicted from the results at 600 cycles, since the course of the attenuation is similar for all frequencies within the range used for the measurements.

The phase profiles were measured with the help of a pressure probe. Its form is indicated schematically in Fig.14. The horizontal part is streamlined. A gauze-covered boring in the center serves as sound pick-up. This boring is five diameters behind the tip of the probe. At this point the flow noise is smallest and the signal-to-noise ratio greatest. The probe is moved through the duct perpendicularly to the absorber surface and the phase angle is registered. From equ. (10) the measured phase angles were transformed into positions of equal phase.

Fig.15 shows phase profiles measured for downstream propagation with various flow velocities at a position of about 40 cm from the duct entrance. The profile for $V_m = 0$ m/sec was

used already in equ.(10) as initial profile $\varphi_o(y)$. The glancing angle ψ in the measured profiles has the following dependence:

V_m	0	11	25	45	55	m/sec
ψ	23^o	28^o	32^o	40^o	47^o	

Whereas the calculations in the foregoing section yield a decreasing angle for increasing flow velocity, the measurements show clearly an increase of the angle ψ with increasing velocity. It must be taken into consideration however, that the influences of the flow profile and of the absorber nonlinearity cannot be separated in the measurements. The nonlinear increase of the flow resistance of the absorber, discussed in paragraph 2, I, results in an increase of the glancing angle of the initial profile. The two causes for the change of the wave form, namely flow profile and nonlinearity of the absorber, are opposite in their effect. Since the calculations in the foregoing section show only a small variation of the glancing angle by the flow profile, the influences of the nonlinearity will prevail. The small influence of the flow profile on the glancing angle for downstream propagation is indicated already in Fig.10, where the only corrections for convection and nonlinearity result already in a velocity-independent attenuation for this direction of propagation.

In the case of upstream propagation the measurements show similar deformations of the wavefronts as were obtained by calculation. Fig.16 shows phase profiles for the flow velocities 11, 25, and 55 m/sec at a position 20 cm from the signal source. A distinct deformation appears only for velocities of about 50 m/sec. A double curvature of the phase profile is caused by the opposite directions of the curvatures of the initial wave front and of the flow profile. The phase profiles have reached their final forms at a distance of about 40 cm from the signal source. For this position the flow profiles differ strongly from each other for different flow velocities.

There is no more similarity with the profile for air at rest. Equation (9) for glancing angle and absorber characteristics is no longer valid.

By comparison of the measured phase profiles with the calculated ones it follows, that the calculation yields the general forma of the profiles, for other parameters of flow velocity and position however. The fact that in the duct the cross dimensions of the flow profile are not great compared to the wavelength results in the principal difference, that in contrast to the calculations there are stable forms of the wavefronts in the duct. These stable wavefronts are built up after a short distance of travel and do not change during further propagation. These waves then propagate with a phase velocity nearly equal to the sum $u_o + V_m$.

IV. Computation of the Change in Attenuation.

An approximative computation of the change of attenuation may be derived by the definition $\alpha = -dN/N$ of the attenuation, where N is the acoustic power through the duct and -dN is the absorbed power per unit length. -dN depends on the energy component $E_\perp$ of the sound field, which is the energy flux normal to the wall. $E_\perp$ is calculated using an equation of Ribner [4], who determines the energy component of a sound wave perpendicular to a flow with velocity V (Mach number $M = V/c$), when flow and wave fronts include an angle γ in terms of the equation

$$E_\perp = \frac{\bar{p}^2}{\rho c} (1 - M \sin\gamma)\cos\gamma \quad . \tag{11}$$

In the case at hand with curved wave fronts and inhomogeneous flow an integral mean of this equation over the height of the duct is taken. For high flow velocities with leading phase near the absorber the sign of $\cos\gamma$ is changed. In the evaluation of the absorbed energy $|E_\perp|$ can be used however. The energy flux density normal to the wall is therefore proportional to

$$|E_\perp| \sim \left| \int \frac{\bar{p}^2}{\rho c} \left\{ 1 - M(y)\sin\gamma(y) \right\} \cos\gamma(y) dy \right| \quad . \tag{12}$$

For the numerical evaluation of this equation the integral is approximated by a sum and the values of $M(y)$ and of $\gamma(y)$ are taken from the measurements. The following relative values of $E_\perp$ are obtained:

-V	11	25	45	55	m/sec
$E_\perp$	1,00	1.27	1.44	2.03	

By the course of $E_\perp$ with V the increase of attenuation is depicted as expected from Fig.10 with increasing value of flow velocity. From this dependence a correction of the measured attenuation could be derived taking account only of the change of the phase profiles in the flow. The correction for the non-linearity of the absorber can be combined by considering the change of the coefficient of absorption. The following relative values of the absorption coefficient are computed from the measurements of the flow resistance:

V_m	0	11	25	45	55 m/sec
$\frac{A_{V_m}}{A_o}$	1	0.95	0.86	0.79	0.63

By definition of the absorption coefficient A the absorbed energy is

$$E_{abs} = E_\perp \cdot A_{V_m} \quad .$$

Applying this combined correction on the measured attenuation per wavelength leads to a good agreement of the corrected attenuation with that measured for air at rest. The influence of flow is eliminated within deviations smaller than 5% for both directions of the signal relative to the flow. These deviations are within the accuracy of measurement.

As a conclusion it can be stated, that the attenuation is changed by convection of the wave for both directions of propagation. For downstream propagation an additional change comes

from the nonlinearity of the absorber. For upstream propagation a third variation results from the deformation of the wave fronts. This variation can neutralize or even overcompensate the loss in attenuation due to the nonlinearity.

§ 3. Experiments Concerning the Sound Amplification with Helmholtz-Resonators.

I. Summary of the Sound Amplification.

The following part of this paper deals with the amplification of an acoustic wave in a duct coated with Helmholtz-resonators. The resonators are arranged on one side of the duct in rows of three resonators tuned at 800 cycles. The distance L between two adjacent rows in the diredtion of the flow is 33 mm. Former investigations with these resonators (F.Mechel [1]) detected an amplification of the input signal for certain frequency bands. The maximum of the amplification obtained was 10 dB/m. The frequency f_a of maximum amplification varied with the flow velocity V_a according to the equation

$$V_a = \frac{u_o}{2} \left(-1 + \sqrt{1 + \frac{4L}{u_o n} fa}\right) \qquad (13)$$

The ranges of amplification follow one another for a fixed flow velocity according to the running number n. In the cited paper the sound amplification was explained in analogy to the electromagnetic traveling-wave tubes. It was proved analytically, that amplification in ducts with periodic subsequence of different wall impedances is possible.

The paper at hand deals with measurements, which help to explain the sound amplification in terms of fluid mechanics as an interaction of the sound field with the turbulence pattern.

II. Experiments with Helmholtz-resonators.

A prerequisite for the following investigations is a detailed knowledge of the flow in the duct and at the necks of the resonators. Measurements were made with the help of the hot-wire anemometer mentioned above. The hot-wire probe allows for measurements of the turbulent and of the acoustic velocities without disturbing the velocity fields. Essentially two quantities were measured:

a) mean flow velocity V
b) root mean square of the turbulent fluctuations.

The flow in the duct with the resonators has a turbulence level on the axis of the duct of 4%. Towards the wall with the resonators the turbulence increases to an amount of 7 to 10% near the necks of the resonators. In the rigid zone between two adjacent necks the turbulence decreases. Therefore a spatially periodic structure of turbulence is found at the wall containing the resonators. The periodicity of turbulence is only present in a layer about 7 mm thick as indicated in the turbulence profiles of Fig.18. The increase of turbulence at the necks of the resonators is caused by the sharp corners of the necks. It will become important later that the necks are positions, where energy of the d.c. flow is converted into turbulence energy.

The frequency analysis of the turbulence on the axis of the duct reveals no enhancement of the resonance frequency of the resonators. By an analysis with constant filter bandwidth one finds a drop of the turbulent velocities with 5 dB per octave (Fig.19). Close beneath the neck of a resonator the resonant frequency is increased about 1.6 dB. This weak influence of the resonators on the turbulence, when they are not excited by an acoustic signal, can be explained by the smallness of the pressure field associated with the turbulent velocity fluctuations and by the ineffectivity of the excitation of the resonators with high Q-value by the turbulent pulses with statistical phases.

According to the different structures of the wall with the resonators and the smooth wall on the opposite side of the duct the mean flow profile is nonsymmetric with respect to the axis of the duct. The mean flow is weakly periodic along the duct. This spatial periodicity is greatly enhanced under conditions of amplification (Fig. 25). The interaction of the resonators with the turbulence becomes great however for some flow velocities, where the duct is self-excited. In this case the resonators are excited by the eddies in the flow and the eddies in turn are stabilised by the oscillation of the resonators. Thereby sound is generated and radiated. Frequency analysis in this case shows a spike of about 14 dB above flow noise. If an additional acoustic signal of a different frequency is fed into the duct, the self-excitation can be suppressed completely by increasing the signal amplitude. The frequency analysis now shows a spike at the signal frequency.

The results of the frequency analysis are plotted in Fig.20 for the two cases. By adding the signal the self-excitation of the resonator is disturbed and the generation of eddies at the corners of the necks is controlled by the oscillation of the resonators but now with the frequency of the signal. By this means the spectrum of self-excitation can be influenced by an added signal.

Here it becomes necessary to deal with the difference between sound and synchronised turbulence as it must be assumed in the case of self-excitation. In the sound field the pressure p and the particle velocity v are connected with one another by the characteristic impedance Z of the medium: $p/v=Z$. Sound waves propagate with the velocity $c = (\varkappa RT)^{1/2}$, where $\varkappa$ is the adiabatic exponent, R the gas constant, T absolute temperature. For synchronised turbulence generated by viscous forces the ratio p/v is smaller by orders of magnitude. As compared with a sound field the pressure is very small. Turbulence has no characteristic propagation velocity, it travels with mean flow velocity V. Because of the lack of

compression of the medium turbulence does not radiate. Monochromatic turbulence, which has similar velocity fluctuations as an acoustic wave, may be called pseudo-sound. Sound and pseudo-sound can be separated in the measurements because of their difference in associated pressure and propagation velocity

The ratio p/v of turbulence was compared with that of sound by detailed measurements. The pressure field was measured by the pressure probe of Fig.14. Its shape guarantees a reliable measurement of the pressure. Velocity fluctuations were measured by the hot-wire probe. The outputs were filtered with a bandwidth of 10 cycles. The acoustic signal was adjusted for equal particle velocity with that of the turbulent fluctuations. For equal a.c. velocities of sound and turbulence the following ratios for the acoustic pressure p_s and the pressures associated with turbulence p_t were measured in a rigid duct:

Mean flow velocity	20	40	60	m/sec
20 log p_s/p_t	37	29	22	dB

The associated turbulent pressure increases with increasing mean flow velocity, since the flow becomes more and more compressible. For the following measurements the mean flow velocity was 45 m/sec. There is no self-excitation for this velocity. Fig.21 shows the results of measurements performed to determine the synchronization of the turbulence. Third-octave analysis were made of the turbulence with a signal of maximum amplification present and without a signal respectively. The energy contents of the third-octave ranges was computed from the output of the filter and the difference of these energies with and without a signal was plotted as function of frequency. The curve makes clear how by synchronization part of the turbulent energy, especially that of the lower frequencies, is fed into the frequency band of the amplified signal. In this frequency band the particle velocity of the signal does not simply superimpose to the flow noise but it influences also

the spectrum of turbulence generated at the necks of the resonators. For the frequency of amplification pseudo-sound is generated at each neck of the resonators.

As a further experiment in connection with the synchronization the particle velocity was measured without flow below the neck of the first resonator of the duct for signals with different frequencies and constant level. The results are entered as circles in Fig.22. Because of the high attenuation of the signal at resonance frequency only a small increase of the particle velocity was found at resonance. The crosses represent the value of the particle velocity measured in the neck of a resonator for signals of 0.8 and 1.3 kc with a superimposed flow of 45 m/sec velocity. Here sound and pseudo-sound were measured together. The dashed curve in that diagram represents the frequency response of the turbulent velocity without an acoustical signal. The amount of sound plus pseudo-sound is distinctly greater than the turbulence at the corresponding frequencies. This can be explained by synchronization with energy-withdraw from the neighbour frequencies.

Since the pseudo-sound moves with the mean flow velocity, it must follow the isotachs of the flow. It does not fill up the whole of the cross-section of the duct as the sound field does, The amplitude of the pseudo-sound decreases quickly with increasing distance from the wall with the resonators. The zone of pseudo-sound has a mean thickness of 7 to 10 mm. The average "life" of the eddies of pseudo-sound, which interfere with the natural turbulence, will be discussed later.

Fig.23 shows the directivity of the turbulent velocities closely upstream and downstream from the neck. For these measurements the directional selectivity of the hot-wire probe was used, which registers preferably velocity fluctuations lying normal to the wire. The directional characteristic of the probe is similar to that one of a dipole. As far as the small accuracy of these measurements allow a conclusion, pseudo-sound generated at the resonator under test is measured only at the downstream corner of the neck as follows from a comparison of the measurements with and without a signal present. This component of

pseudo-sound is plotted separately in Fig.23a. The pseudo-sound component includes an angle of 40 degrees with the normal on the wall. This indicates, that the a.c. flow emerging from the neck is blown away by the mean flow. The a.c. flow is perpendicular to the wall for air at rest.

The generation of pseudo-sound at the resonators is the cause of the sound amplification. An indication of this behaviour can be found from former measurements [1] with weakly damped Helmholtz-resonators. The damping was realized by two methods

a) the resistive gauze was glued on the side towards the duct of the necks
b) the same gauze was glued on the backward side of the necks.

In case a) the wall of the duct becomes smooth, the generation of eddies at the corners of the necks is suppressed in a high degree. Correspondingly the frequency response of the duct attenuation shows no pecularities. In case b) the generation of eddies is not disturbed unless a decrease of the particle velocity in the necks. The frequency response of the duct attenuation reveals bands of small deattenuation coinciding with the bands of amplification of the undamped resonators.

III. Mechanism of Amplification.

With the help of the absolutely calibrated hot-wire anemometer the cross-sectional distribution of the turbulence was measured at different positions along the duct. By these measurements the change of turbulence by the superposition of the signal should be recognized. The signal had the constant frequency of the maximum amplification at the flow velocity of 45 m/sec. Because of the calibration of the probe the measurements must be performed with a broad frequency band allowed on the receiver side. Frequency analysis showed however, that any change of the turbulence was caused essentially by the spike of the pseudo-sound.

The difference of the root mean square of the turbulence with and without the amplified signal is plotted in Fig.24 into a sketch of the duct. The fact that this difference is caused only by the pseudo-sound and not by the a.c. velocity of the sound field directly is proved by the following arguments:

a) Upstream of the first resonator the difference is zero, although the signal is present.
b) The amplitude of the difference is limited spatially in transverse direction.
c) The maximum lies on the isotachs (Fig.25) of the mean flow.
d) By the strong interaction with the natural turbulence the difference decreases in such a rate, that it would disappear after a propagation of about 5 cm.
e) A non-vanishing difference could be measured only for signal frequencies near the amplification maximum.

The meaning of item e) will become clear when the phase relation between sound and pseudo-sound will be discussed.

First a short discussion of the results plotted in Fig.24: The resonators were numerated with k = 1, 2, ... in the direction of signal propagation,

k = 1 On the upstream side of the first resonator the difference of the turbulence measurements is zero. There is no pseudo-sound. Turbulence is synchronised in the neck of the resonator. Here the region of vanishing difference is sharply limited towards the axis of the duct. Behind the resonator the zone of pseudo-sound moves along an isotach with mean flow velocity.

k = 10 The structure of the zones of pseudo-sound has reached its final form. On the upstream corner the pseudo-sound coming from the resonator k = 9 is measured. New generation takes place in the neck of the resonator. Behind the resonator both the regions of pseudo-sound can be found with a weakly marked separation between them. During further propagation the older eddy dissolves.

k = 11 The same cycle takes place.

An important conclusion is, that pseudo-sound is localisable during its propagation. Pseudo-sound generated at the resonator k can interfere with that generated at the resonator k+1.

Considering the interference and the phase relations between sound and pseudo-sound their different propagation velocities become important. The following symbols are used:

	velocity	frequency	wavelength
Sound	u	f	$\lambda_s = u/f$
Pseudo-Sound	V	f	$\lambda_p = V/f$

It is important to state, that the phase of the resonator oscillation is controlled by the signal. The phase lag between two adjacent resonators with the distance L is

$$\varphi_{k+1} - \varphi_k = 2\pi \frac{L}{\lambda_s} = 2\pi \frac{Lf}{u} \tag{14}$$

A phase lag between the resonators may be contributed to the pseudo-sound in the same manner:

$$\psi_{k+1} - \psi_k = 2\pi \frac{L}{\lambda_p} = 2\pi \frac{Lf}{V} \tag{15}$$

For simplification the phase angles at the resonator k shall be zero: $\varphi_k = \psi_k = 0$. In order that the phase angle between sound and pseudo-sound at the resonator k+1 be the same as at the resonator k, the relation

$$\psi_{k+1} - \varphi_{k+1} = 2\pi n \qquad n = 1,2 \ldots \tag{16}$$

must hold. It follows

$$\frac{Lf}{u} = \frac{Lf}{V} - n. \tag{17}$$

By this equation two values of f and V (periodic in n) are distinguished, for which the superposition of the pseudo-sound from k and from k+1 results in an increased amplitude at the position k+1. For the same velocity V but other frequencies f the result of the superposition is smaller and for a phase lag of π it results in an extinction of pseudo-sound. From equation (17) follows a frequency response of the distinguished values of V for maximum amplification. Replacing λ_s by phase velocity u and frequency f and taking into account, that the phase velocity is $u_V = u_o + V$, one has

$$V_a = \frac{u_o}{2} \left(-1 + \sqrt{1 + \frac{4L}{u_o n} fa}\right) \qquad (18)$$

This is the equation derived by F.Mechel in a similar way, when he compared the sound amplification with the amplification in traveling-wave tubes. The values V_a and f_a of maximum amplification coincide with those calculated from equation (18).

Equation (17) leads also to a simple evaluation of the frequency response of the amplification near an amplification maximum at the frequency $f_{V,n}$. If in the derivation of equation (17) instead of exact synchronism a phase difference $\Delta\varphi$ is permitted, one obtains for a certain V

$$\Delta\varphi = 2\pi n \left(\frac{f}{f_{V,n}} - 1\right) \qquad (19)$$

The phase relation between sound and pseudo-sound at a fixed moment is indicated in Fig.26. At the first resonator $\varphi_1 = \psi_1 = 0$ was assumed. The sketch is valid for the amplification with n=1, which lies for example for V = 45 m/sec at f = 1.35 kc. Equality of phases for sound and pseudo-sound is found near the necks of the resonators. Here they interfere with one another. The strength of interference and the amplification resulting thereof can be seen from Fig.27. There the distribution of the a.c.pressure is plotted as measured with the

pressure probe mentioned above. For comparison the distribution of the acoustic pressure without flow is entered too.

The pressure curves yield an increase of about 4 % between two adjacent resonators for all distances from the wall. This results in an increase of 10 dB/m in the maximum of amplification, which agrees with the former measurements at these values of V and f. The curves in Fig.27 are relative variations of alternating pressure.

The partial or complete extinction of pseudo-sound occuring for a phase lag between the eddies generated at the resonators k and k+1 and meeting one another at k+1 can be seen from Fig.28, where the frequency responses of pseudo-sound and turbulence are represented. In this experiment the alternating velocities were measured close behind a neck by the hot-wire probe, whose output was filtered with 10 cycles bandwidth. The frequency of the superimposed acoustical signal varied in synchronism with the filter center frequency. The curve shows two maxima corresponding to the amplification frequencies $f_{V,1}$ and $f_{V,2}$. At the same time the frequency distribution of the natural turbulence is entered. The increase at $f_{V,2}$ is smaller because of the phase angle 4π of the pseudo-sound between two resonators as compared to 2π for $f_{V,1}$. Therefore the trouble incidence of the eddies of pseudo-sound for interference with the natural turbulence becomes greater.

The measurements can be summarised as follows: Synchronised eddies are generated at each resonator for each frequency, but only for frequencies of amplification, stable, long range pseudo-sound pulsations are possible, which are all over the length of the duct in a constant phase relation to the signal wave. Therefore amplification as an interference over the whole length of the duct is possible only for these frequencies.

With the help of a coupling factor to be derived from the measurements and the interrelation between a frequency shift and the associated phase lag between two regions of pseudo-sound

$$\Delta\varphi = 2\pi\, n\left(\frac{f}{f_{V,n}} - 1\right) \qquad (19)$$

the amount and frequency response of the amplification can be calculated. The superposition of the normalised signal wave

$$A_s = \sin \omega t$$

with the coupling part of the pseudo-sound having a phase lag $\Delta\varphi$

$$A_p = K \sin (\omega t + \Delta\varphi)$$

results in

$$A = \sin \omega t + K \sin (\omega t + \Delta\varphi)$$

$$A = K[(\tfrac{1}{K} + \cos\Delta\varphi)\sin \omega t + \sin\Delta\varphi\cos \omega t] \qquad (20)$$

Elimination of the time dependent term leads to the amplitude for the two superimposed oscillations

$$A = (1 + K^2 + 2K \cos\Delta\varphi)^{\frac{1}{2}} \qquad (21)$$

That is the amplitude of the response of a probe after a distance of one resonator. For a number of 28 resonators per meter the increase in amplitude per meter will be

$$A' = (1 + K^2 + 2K \cos\Delta\varphi)^{14} \qquad (22)$$

Introduction of equation (19) leads to the frequency response of the amplification

$$D(f) = 280 \log \left\{ 1 + K^2 + 2K \cos \left[2\pi\, n\left(\frac{f}{f_{V,n}} - 1\right)\right]\right\} \frac{dB}{m} \qquad (23)$$

Equation (23) was evaluated for n=1, $f_{V,1}$=1.35 kc and a flow velocity V = 45 m/sec. The calculated curve is compared with the measured one in Fig.29. The poor agreement for low frequencies comes from the resonance lying close by, as it will be soon explained.

The foregoing results allow for an explanation of the amplification mechanism in terms of fluid mechanics. The first question in connection with this amplification is, where the additional acoustic energy comes from. The answer must be: from the kinetic energy of the flow. The next question then will be, by which mechanism is kinetic flow energy converted into acoustic energy.

It is well known, that there is no direct energetic interference between flow and acoustic wave unless at very great amplitudes. Our measurements however yield the result, that for very high signal levels the amplification decreases. Therefore it is necessary to assume some vehicle, which transports the energy from the flow to the acoustic wave. This connecting link must be sensitive to acoustic vibrations but also must be able to withdraw energy from the flow.

This function can be taken over by the turbulence. Since the energy exchange is unidirectional, the turbulence cannot be statistical in its phases relative to the sound wave, but must be periodical with the signal frequency. It must be synchronized by the signal. This synchronization was checked in the foregoing measurements.

By what means may these velocity fluctuations of the pseudosound be excited? It is known from aerodynamics, that the turbulence in a duct may be influenced to a high degree by outflow or inflow through the walls. The onset of turbulence at high flow velocities can be suppressed by suction velocities which are smaller by a factor of even 10^{-4} than the velocity of the flow to be influenced. Now the necks of the resonators are places of periodic suction and blow out. The formation of eddies at the neck corners can be controlled by the oscillation of the resonator. The energy fed to the eddies comes from the flow; the control itself demands nearly no energy. The eddy once developed in the rhythm of the resonator oscillation will float with the streaming.

The term "eddy" above shall stand for an individual velocity pulsation of some manner undefined until now. In order to clarify the shape of these "eddies" the local phase distribution of the

alternating velocities was measured in the neck and immediately below it for conditions of maximum amplification. The result was, that below the neck on both the upstream and downstream sides the instantaneous flow velocity is greater than the mean value for the suction phase of the resonator. An evident explanation for this behaviour is, that by the suction of the resonator the d.c. flow profile is shifted instantaneously towards the wall containing the resonators. At the same moment higher velocities will be measured at some point below the resonator due to this shift. At the outblow phase of the resonator the isotachs of the d.c. flow are moved away from the resonator correspondingly. This instantaneous lift and drop of the flow profile has a lateral extension of about 7 mm from the corners of the neck. These measurements show, that the synchronized turbulence is rather a pulsation of the local flow velocity than rotational eddies. It gives an explanation also for the fact, that the transversal extension of these pulsations is only small, since the instantaneous influence on the flow profile can extend only over a small region.

From these instantaneous deformations of the flow profile must be clearly distinguished the fact, that the mean flow profile averaged over the time is changed also in presence of an amplified signal. Corresponding flow profiles are shown in Fig.30, where full lines represent the distributions with signal and the dashed lines without. The measurements were performed below a neck and between two of them. With a signal present the mean flow velocity gradient becomes greater near the resonators. That is associated by greater viscous forces tending to decelerate the flow. Thus from these measurements it can be seen directly how by the amplified signal the mean flow energy is decreased.

The instantaneous variations of the flow profile give rise to the velocity pulsations v of the pseudo-sound. They can be measured at some fixed position behind a resonator with the help of the hot-wire as a velocity sensitive probe. By any pressure sensitive probe one could measure at the same point an alternating pressure also, which is associated to the alternating velocities v of the pseudo-sound in terms of the equation

$$p = A \cdot \varrho \frac{\partial v}{\partial t} + B \cdot \frac{\varrho}{2} v v \quad , \qquad (25)$$

if the amplitudes are small compared with the mean flow velocity V. Here A and B are factors depending on the form of the probe. If the probe picks up the pressure in the stagnation point, B is great, while if the opening lies on the side of the probe and flush with the wall, A is the significant term.

Now the opening of the Helmholtz-resonator is such a pressure sensitive probe. Since the opening is flush with the wall, it reacts upon the first term A. This means, that the flow pulsation from the first resonator, controlled by the sound and energy supplied by the flow, may influence oscillations at the second resonator. If the second resonator oscillates already under the influence of the signal wave, the flow pulsation may amplify the oscillations depending on the phase relation between sound and pseudo-sound.

Before discussing the proper phase condition further, reference to Fig.27 shall show, that it is the above pressure component of equ. (25), which excites the resonators to the amplified oscillations. In that graph is plotted the relative variation of the alternating pressure in percents of the mean value at various distances from the boundary of the resonators. The dashed line is for air at rest, the full line for flow plus signal under conditions of amplification. Along the resonators rigid zones between the resonators and nearly pressure release zones below the necks follow one another periodically. Just below the boundary the pressure of the sound wave is well defined by the wall impedance. The pressure must break down below the necks. Nearer to the axis of the duct the influence of the wall impedance comes to a mean value. With superimposed flow, however, the amplitude of the alternating pressure just below the neck is greater than the mean value. This is possible only, if there is a pressure component, which is not combined with its corresponding particle velocity via the wall impedance. This is the situation with the alternating pressure connected to the pseudo-sound.

The rate of energy fed from the flow into the sound wave, that is the sound amplification, is proportional to the product of the strength of turbulence generation times the degree of energy recovery at the resonators. In order that the level of

synchronized turbulence be the greatest possible, it is sufficient (for a given shape of the necks), if an arbitrary eddy, generated at the resonator k superimposes cophasally over the eddy generated at the resonator k+1 some time later. This results in the phase condition, that the eddies during their propagation along the resonators must find them all in the same phase of oscillation. From this condition was derived equ. (13). The energy recovery, that is the amplification of the resonator oscillations on the other hand will be greatest, if the associated pressure (equ. (25) term A) of the pseudo-sound coincides in phase with the acoustic pressure below a resonator. Taking into consideration the two facts, first that the alternating pressure of the pseudo-sound has a phase advance of 90 degrees relative to the velocity v and second that the velocity v of the pseudo-sound at a resonator is maximum for the suction phase of the resonator, it follows, that the input impedance of the resonator must be a purely inductive one for optimum excitation.

This additional condition for maximum amplification leads to an explanation for some experimental results. First amplification could be found only for frequencies above resonance, where the resonator impedance has an inductive component. Measurements with quarter-wavelength resonators revealed deattenuation only for frequencies, where the reactance is inductive. Second the amount of amplification in Fig.2 is nearly the same for all frequencies, whereas it should be expected, that it be greatest near resonance, where the oscillation amplitudes of the resonators are greater than for frequencies far from resonance. The strength of pseudo-sound generation varies surely in the same sense as the oscillation amplitudes. The amount of energy recovery however is determined by the character of the resonator impedance. This is a dissipative resistance for resonance and becomes more and more inductive for higher and higher frequencies. The same explanation holds for the deviation of the theoretical curve from the experimental one in Fig.29. The calculations there assume the same amount of energy recovery over the whole frequency range. This assumption must fail for frequencies approaching resonance.

Third the measured flow velocities of maximum amplification are smaller than the velocities predicted by equ.(18) for frequencies near resonance. When approaching the resonance frequency from the side of higher frequencies the phase advance of the acoustic pressure relative to the oscillations of the resonator decreases from 90 degrees towards zero. The inphase condition for the acoustic pressure and the pseudo-sound pressure can be satisfied however, if the maximum of the pseudo-sound velocity has a phase lag relative to the maximum of the suction velocity of the resonator. This phase lag can be achieved by smaller propagation velocities of pseudo-sound, meaning smaller flow velocities. These phase lags between incoming pseudo-sound velocity and suction velocity were detected in the phase measurements mentioned above.

IV. Some Experiments for Upstream Propagation.

Finally some measurements shall be reported for the signal propagating in the upstream direction in the duct with resonators. For this case an amplification as distinctly marked as in the case of downstream propagation could not be found. The frequency response of attenuation in the duct reveals small deattenuation (1 to 2 dB) for the frequencies according to the dispersion curve which was derived in analogy to backward-wave tubes [1]. This deattenuation differs from the amplification for downstream propagation by its great amplitude dependency. Discussing this deattenuation under the aspects outlined above, the following differences can be stated:

a) A synchronized eddy moves opposite to the signal wave. The condition of constant phase before the resonators leads to another dispersion curve of the deattenuation, since now the phase angle of the signal to be amplified between two resonators adds to the phase angle of the pseudo-sound:

$$V = \frac{u_o}{2}\left(1 - \sqrt{1 - \frac{4L}{u_o n} f}\right) \qquad (24)$$

b) Because of the opposite direction of sound and pseudo-sound also the sense of the phase rotation is opposite. At the position of a neck, where sound and pseudo-sound interfere with one another the duration of nearly equal phase is smaller here than for downstream propagation.

c) The spatial distribution of the particle velocity of the oscillation in the neck is influenced by the flow in the way, that it becomes nonsymmetric with respect to the axis of the neck. This dissymmetry is objective however for the interaction with the flow. A measurement of this distribution is given in Fig.31 for a mean flow velocity of 30 m/sec. At the upstream corner of the neck the generation of turbulence will be greatest, there however the particle velocity of the oscillation is smaller than at the other corner.

These arguments indicate a weaker interaction between sound and pseudo-sound and could help for explanation if a long range stable pseudo-sound generation would be prohibited at all. Frequency analysis of turbulence with covarying signal and filter center frequencies as in Fig.28 correspondingly reveal only a small increase for the frequencies of deattenuation, which are to be expected from the dispersion equation for upstream propagation. Such measurements are reproduced in Fig.32.

It can be seen, that also for upstream propagation of the signal interference with the flow takes place in a similar manner as for downstream propagation, because of the unfavourable circumstances there is only a small deattenuation possible however.

References

[1] E. Meyer, F. Mechel, G. Kurtze — Experiments of the Influence of Flow on Sound Attenuation in Absorbing Ducts. J. Acoust. Soc. Am. 30 (1958) 165

F. Mechel — Schalldämpfung und Schallverstärkung in Luftströmungen durch absorbierend ausgekleidete Kanäle. Acustica Vol.10 No.3 (1960) 133

[2] H. Schlichting — Grenzschicht-Theorie. Karlsruhe 1958

[3] K. Schuster — Zur Schallausbreitung längs poröser Stoffe. Akust. Z. 4 (1939) 335

[4] H. Ribner — Reflection, Transmission and Amplification of Sound by a Moving Medium. J. Acoust. Soc. Am. 29 (1957)435

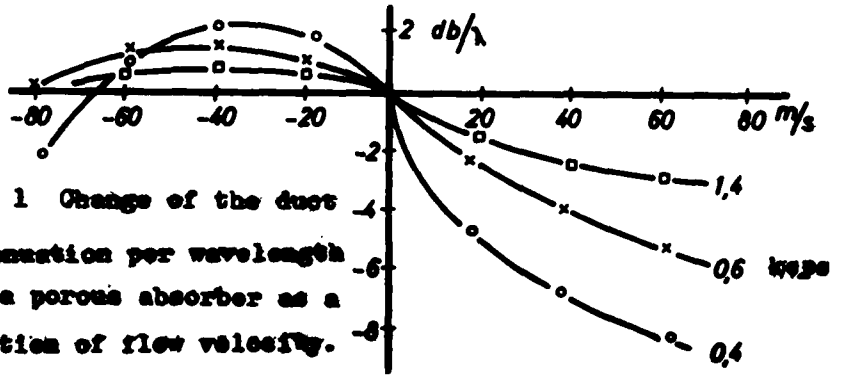

Fig. 1 Change of the duct attenuation per wavelength for a porous absorber as a function of flow velocity.

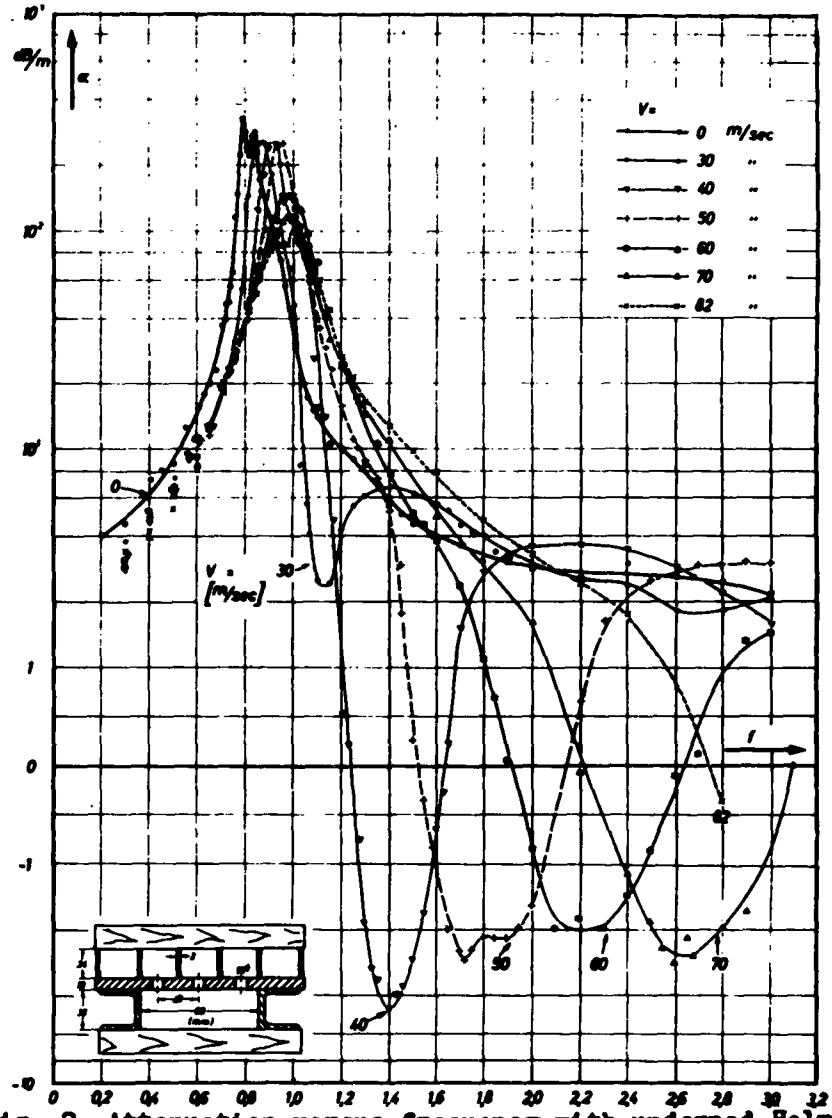

Fig. 2 Attenuation versus frequency with undamped Helmholtz-resonators. Parameter: Flow velocity V = 0.

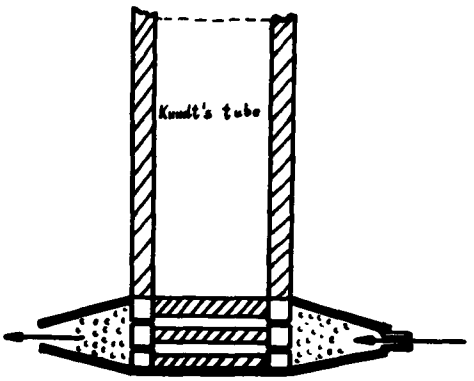

Fig. 3 Measuring chamber terminating the Kundt's tube for the measurement of the impedance of porous materials with superimposed flow.

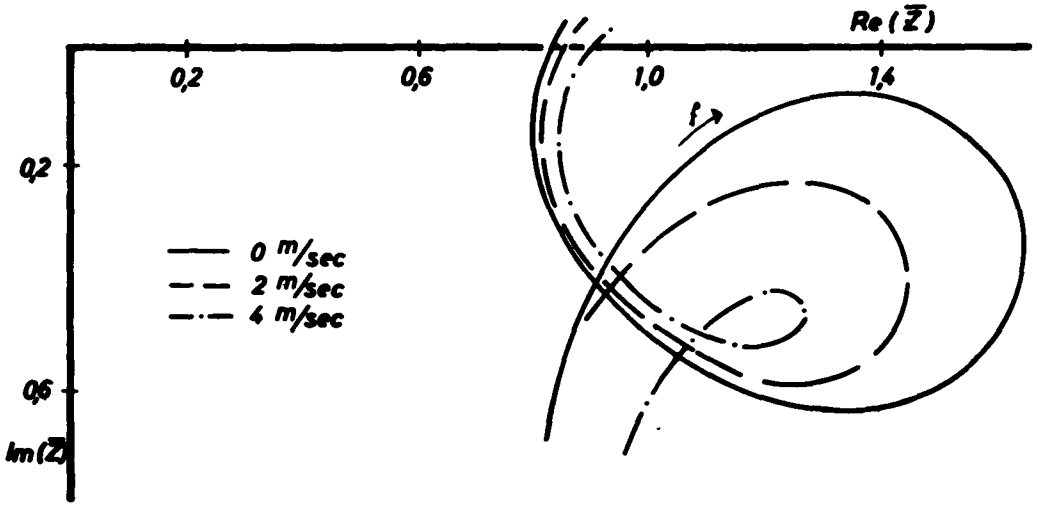

Fig. 4 Frequency response of the impedance for different flow velocities.

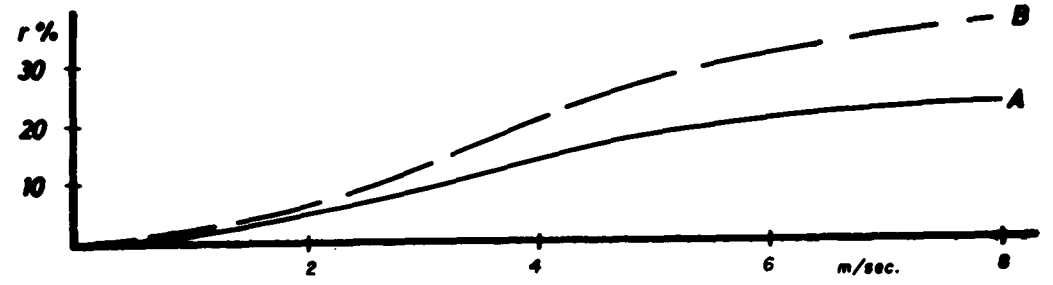

Fig. 5 Measured variation of flow resistance.

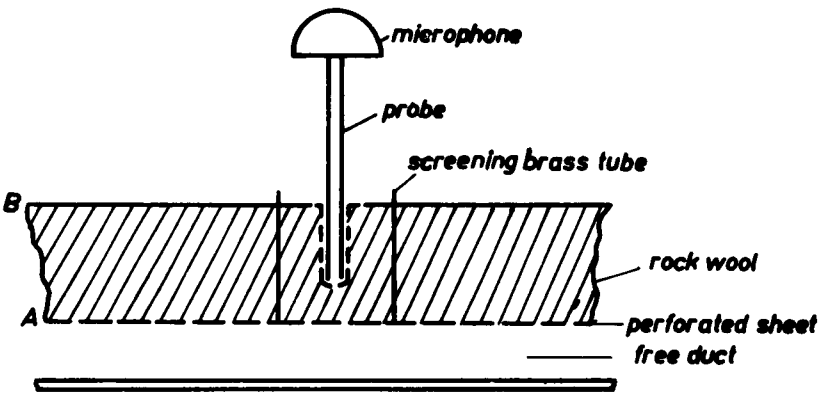

Fig. 6 Arrangement for the determination of the attenuation in rock wool

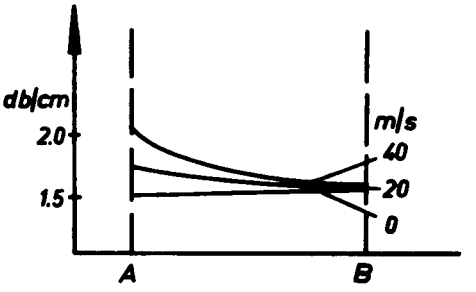

Fig. 7 Change of impedance at various distances from the duct wall

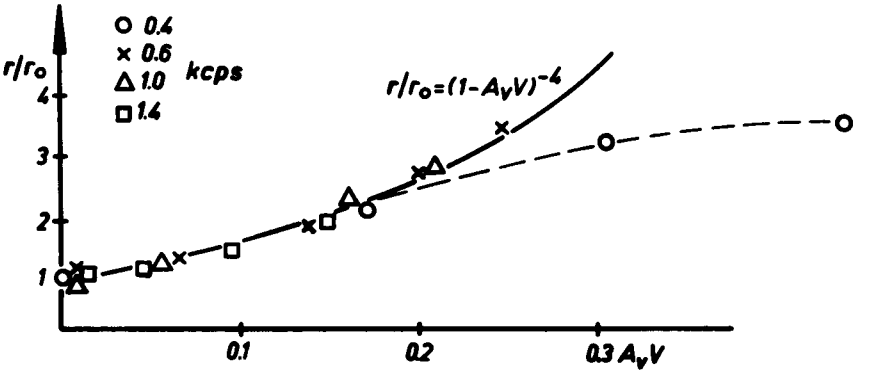

Fig. 8 Change of flow resistance

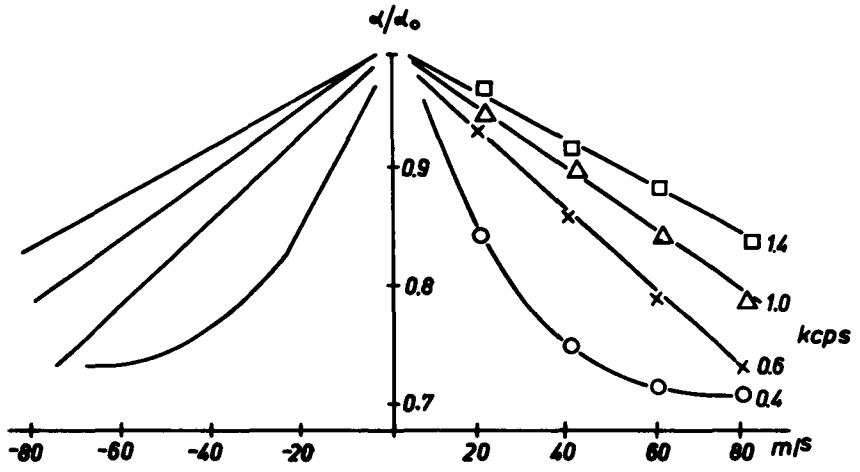

Fig. 9 Relative change of attenuation in the duct caused by a change of impedance of the rock wool.

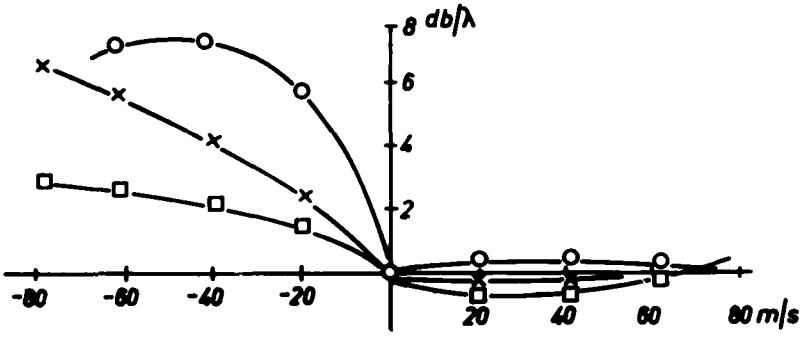

Fig. 10 Values taken from Fig.1 and corrected according to Fig.9.

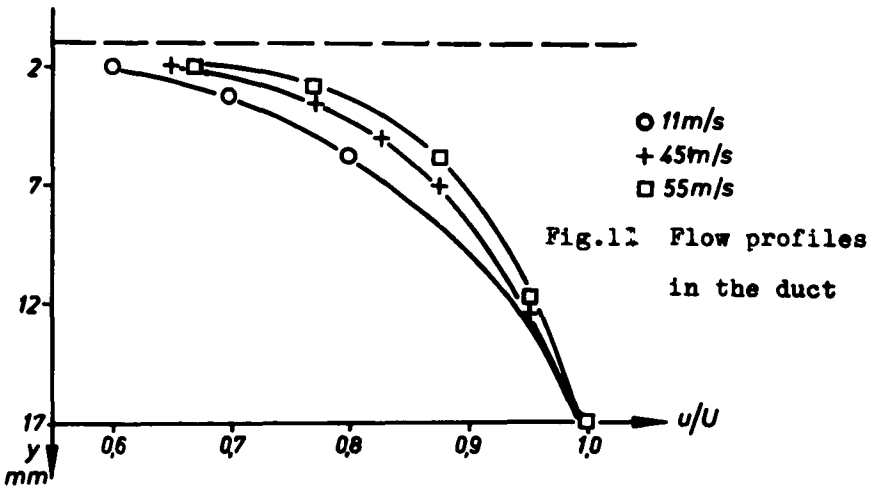

Fig.11 Flow profiles in the duct

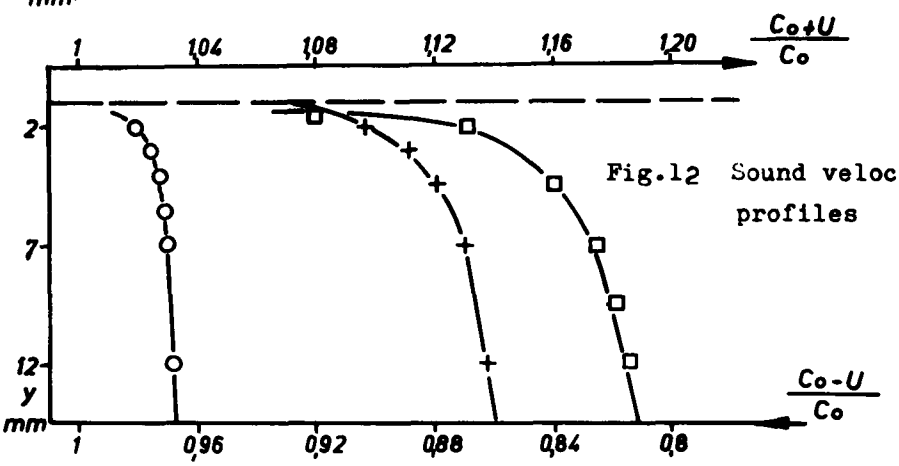

Fig.12 Sound velocity profiles

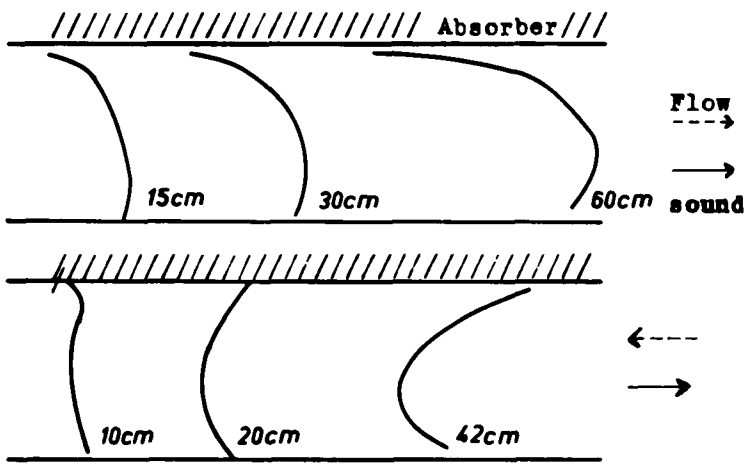

Fig.13 Phase planes for forward and backward propagation

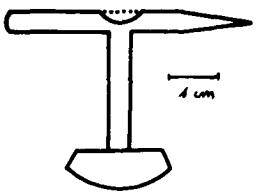

Fig. 14 Dimension of the T-shaped probe.

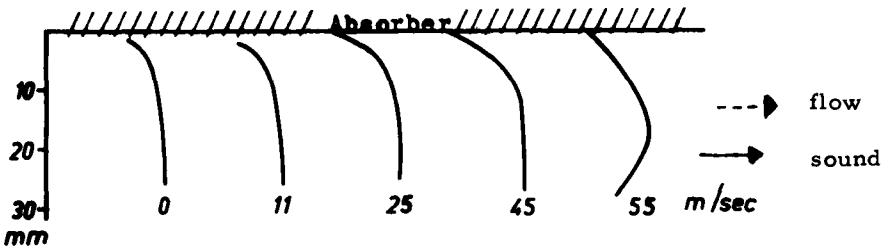

Fig. 15 Phase planes measured for forward propagation 600 cps, distance from signal source 40 cm.

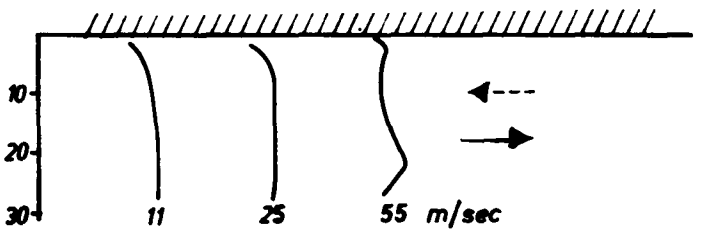

Fig. 16 Phase planes at the entrance into the absorbing duct. (Distance from the entrance 20 cm)

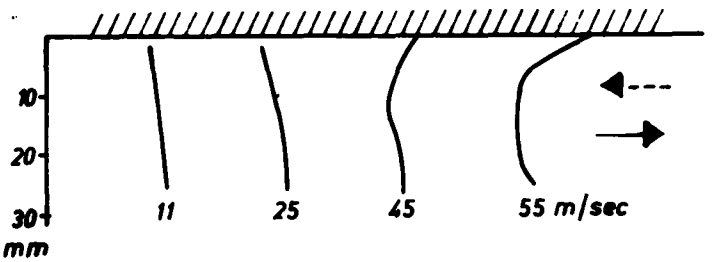

Fig. 17 Final phase planes in the case of sound propagation against the direction of flow.

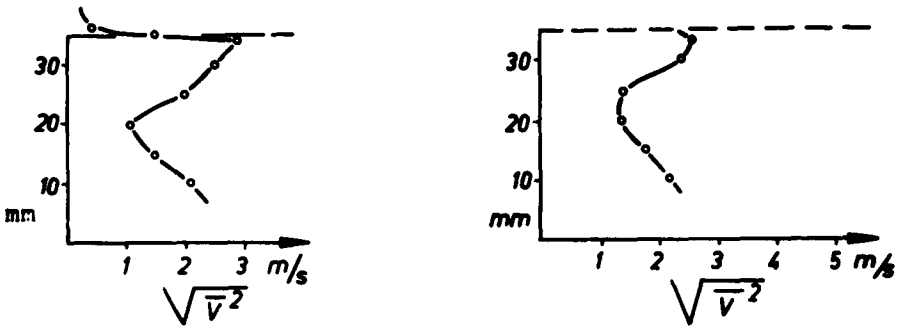

Fig.18 Turbulence-velocity at the neck of the resonator and between two resonators.

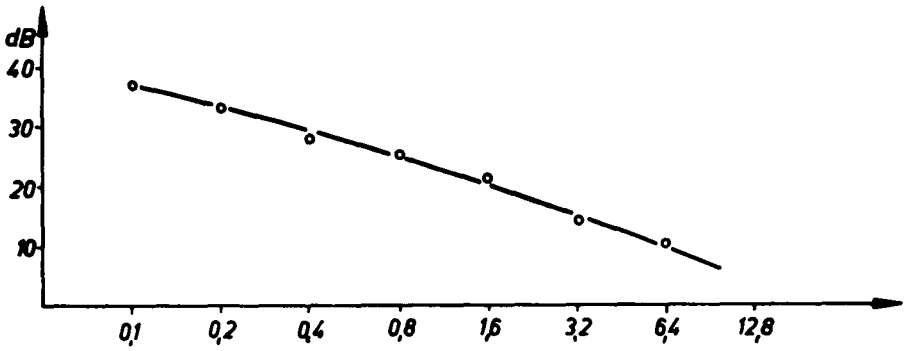

Fig.19 Frequency-analysis of the turbulence-velocity.

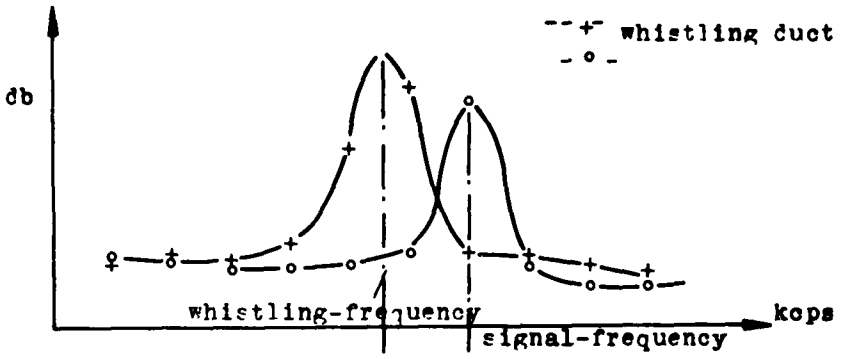

Fig.20 Change of the spectrum of turbulence by supplied sound signal.

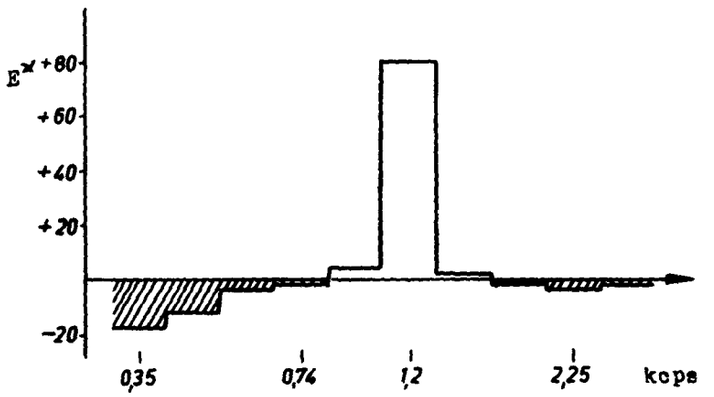

Fig 21 Differences of energie-contents of the third-octave ranges with and without superimposed sound.

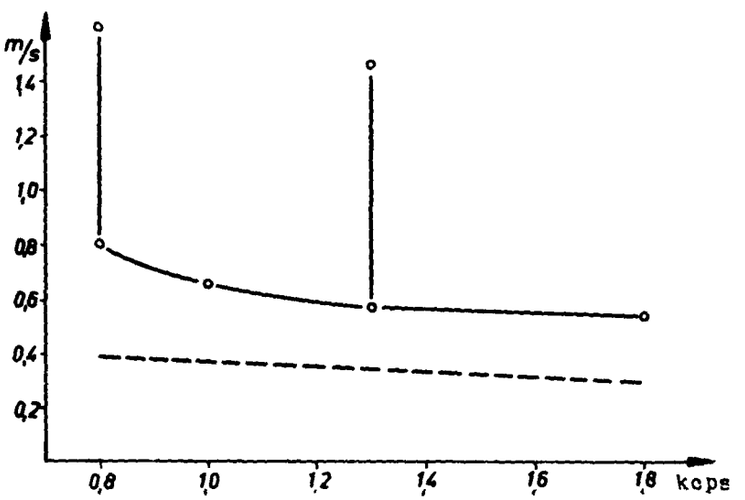

Fig 22 Particle velocity below the neck of the resonator. At 0.8 and 1.3 kcps: with superimposed air-flow.

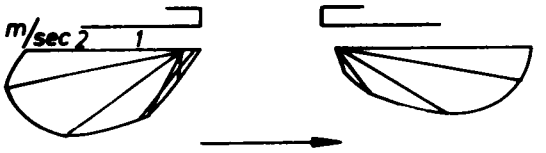

Fig. 23 Directional distribution of turbulence velocity.

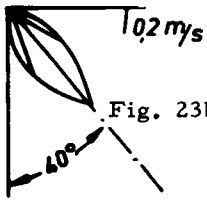

Fig. 23b Part of pseudo sound.

23b

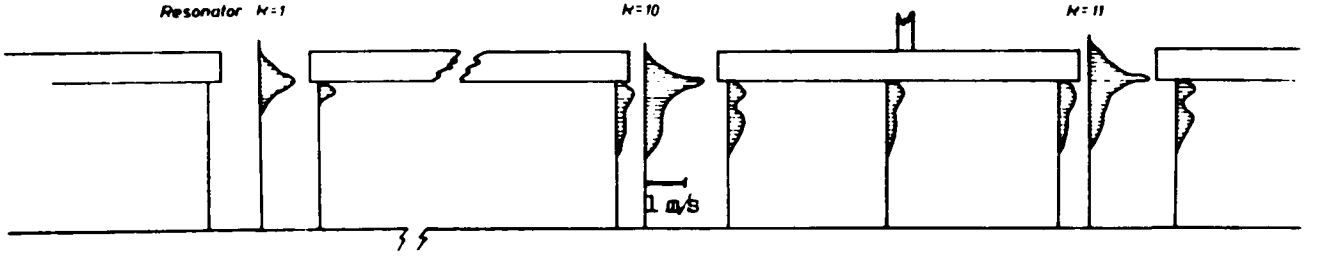

Fig. 24 Pseudo-sound distribution in the duct 0.5 cm = 1 m/sec particle velocity.

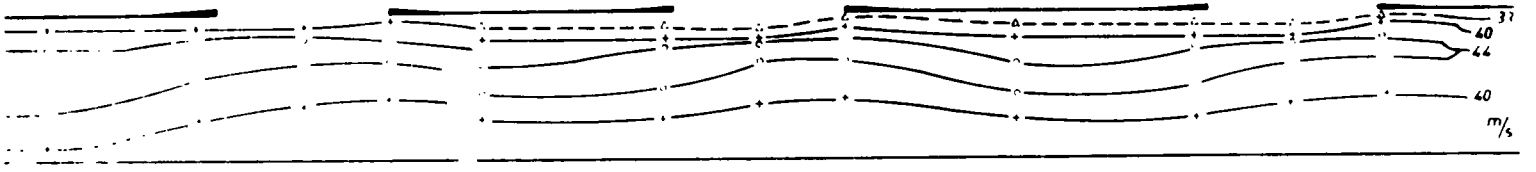

Fig. 25 Isotachs of mean air flow velocity.

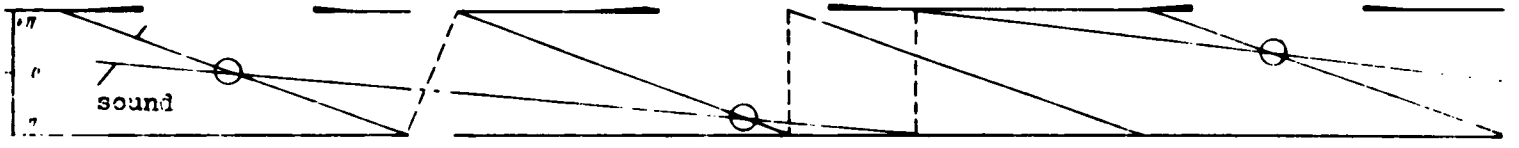

Fig. 26 Phase relation between sound and pseudo sound (wavelength of sound is shortened)

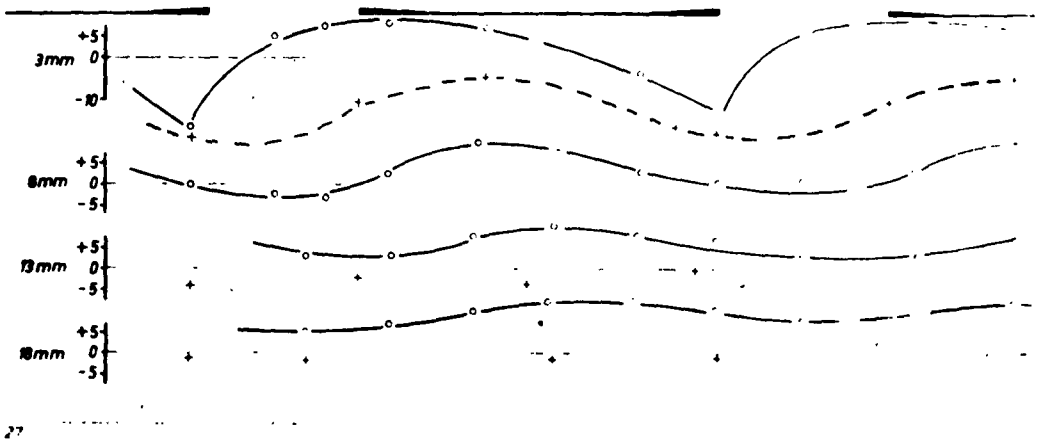

Variation of sound pressure at various distances from the resonator wall.

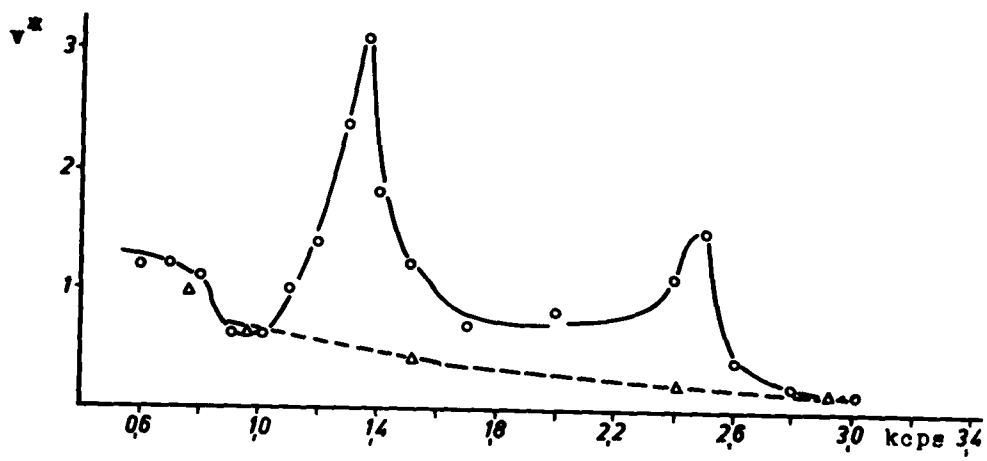

Fig.28 Frequency-analysis of turbulence. The signal frequency is varied in synchronism with the center frequency of the filter.

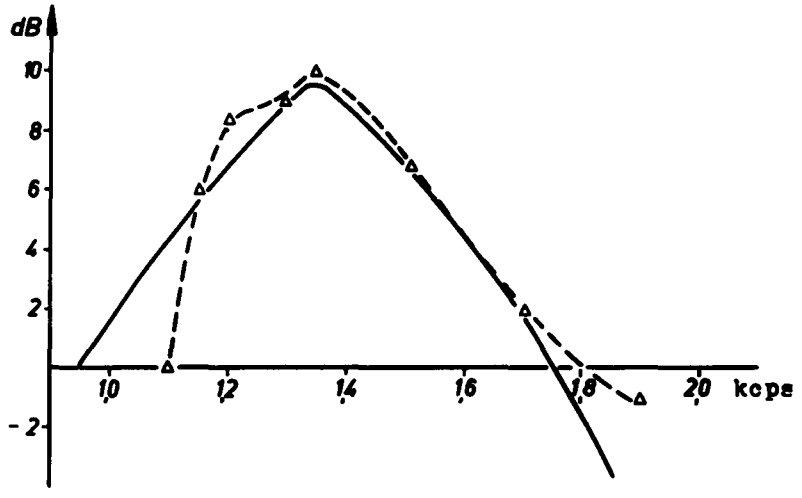

Fig 29 Calculated and measured amplification-range.

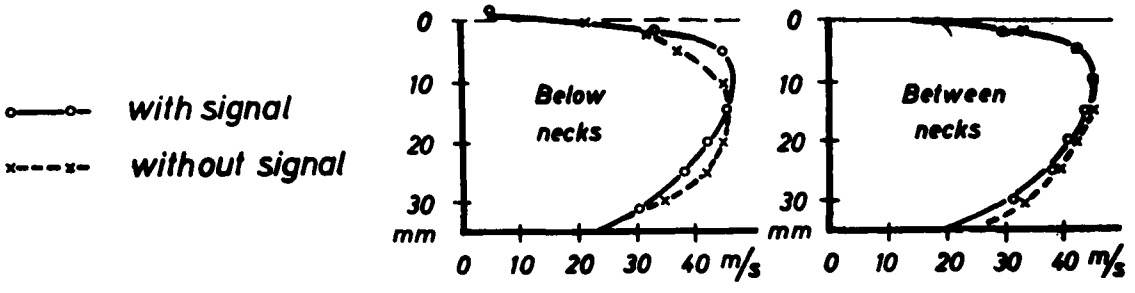

Fig. 30 Profiles of the time-averaged flow velocities with (unbroken line) and without (dashed line) amplified signal superimposed.

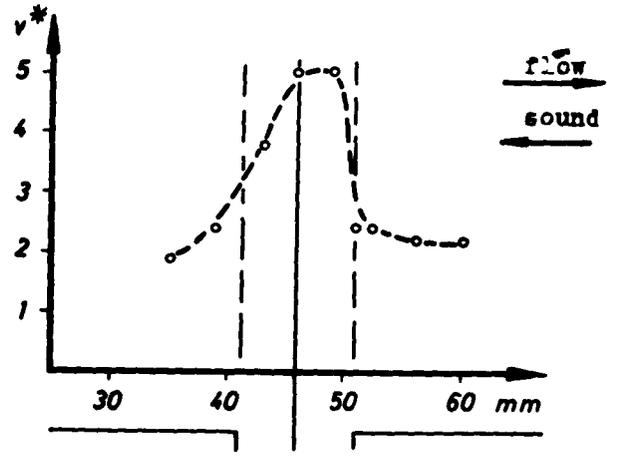

Fig. 31 Local distribution of alternating signal velocities below the neck of a resonator for frequency and velocity of amplification.

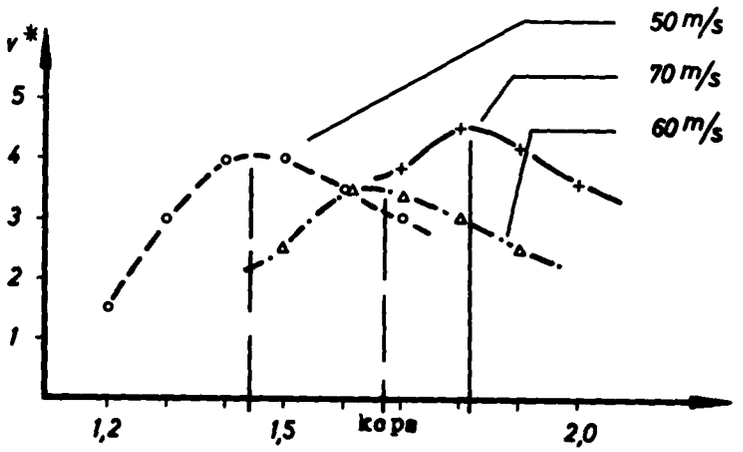

Fig. 32 Frequency analysis corresponding to that in Fig.28 for upstream propagation and different flow velocities

Part B

A New Wind Tunnel for Acoustic Measurements with Flow Velocities up to 200 m/sec.

SUMMARY

A new wind tunnel for acoustic measurements with flow velocities up to 200 m/sec in the test section is described. The available signal -to-noise ratio was increased by careful design of mufflers and flow rectifiers as well as by the development of a small condenser type microphone with low self-noise and small sensitivity to turbulence. Attenuation measurements were performed with an absorber of rock wool using both pure tones and noise as signal. Elimination of the convective effect of the flow upon attenuation allows for separation of the different influences of the flow.

Introduction

At the III.Physikalisches Institut der Universität Göttingen measurements were performed in the past years of the attenuation of air-borne sound in absorbing ducts with superimposed air flow with velocities of up to 80 m/sec. These measurements were to be continued with higher flow velocities. For this purpose the construction of a new wind tunnel was necessary.

§ 1. Design of the Tunnel.

In the preceeding measurements it was found, that one of the most severe experimental problems in connection with acoustic measurements in flows with high velocities is a sufficient signal-to-noise ratio. It can be improved by high signal levels, by a small bandwidth of the receiving system and by reduction of the noise level. As signal generators two loudspeakers of 200 Watts each are used. That is near the limit as well of the technical possibilities as of the level allowed physically, if one wishes to have sine waves in the duct rather than shock waves. The filter output was filtered hitherto with a bandwidth of 6 cycles. Still smaller bandwidth would prohibit measurements in reasonably short times. Therefore it is necessary to reduce the disturbing noise to a level as low as possible. The noise may be divide into one component, which is generated at the microphone (the reduction of this component will be discussed later) and a second part, which is composed of:

1) noise from the blower propagating as air-borne sound in the flow,
2) noise from the flower propagating as structure-borne sound into the measuring path of the duct,
3) noise from the turbulence in the measuring path,
4) noise from the flow outlet into free space, which may propagate into the measuring path either directly in the flow or by cross-talk from the test room.

The outlet noise was reduced by a conical diffuser of 4.5 meters length with a sound absorbing coating on the last 3 meters. The outlet velocity does not exceed 6 m/sec. Cone angles were choosen so, that flow separation in the diffuser was avoided. The pressure recovery for the highest flow velocities amounts to 65 %.

The turbulence level in the measuring path is determined both by the turbulence level of the incoming flow and by the strength of turbulence generation at the walls of the measuring path itself. In order to provide the possibility of measurements, for which a low turbulence level of the incoming flow is a prerequisite, turbulence reduction is performed before the inlet of the measuring path. This reduction is performed by the combination of a contracting cone (area ratio 37) and gauze screens. Contracting cone and screens were designed in a way that 40 dB turbulence reduction was achieved. The flanges for the insertion of the gauze screens and the contracting cone are seen on the right of Fig.1. For full turbulence reduction a section of the duct of at least 1 meter in length should be inserted between the last screen and the cone. In most attenuation measurements the turbulence in the measuring path is determined however by the surface structure of the absorber under test. Full turbulence reduction is not necessary therefore with these measurements. That is why in Fig.1 the duct length between screen and gauze is shorter. Here the principal effect of the screens is to procure an equal flow distribution over the cross section of the duct and to avoid flow separations, which give rise to low frequency pressure pulses.

The muffler for the air-borne sound and insulations for the structure-borne sound coming from the blower were carefully designed. Flanges of soft rubber without metallic junctions were inserted before the muffler and the contracting cone. Cross sections of the muffler are shown in Fig.2. It was postulated, that an attenuation better than 40 dB should be reached for frequencies above 200 cycles with reasonably low pressure loss in the muffler. The final form of the muffler had to

satisfy many acoustic and aerodynamic reclaims inconsistent with one another. Sound attenuation decreases for downstream propagating noise with increasing flow velocity. Therefore 10 m/sec were allowed in the muffler as an upper limit. That leads to large cross-sectional areas. Since the interaction of sound and absorbing walls decreases for high frequencies and large cross sectional areas, the total free cross-section of the muffler must be split up into parallel ducts. These ducts were curved furthermore in order to improve the attenuation at higher frequencies. Splitting up the cross-section of the duct includes the danger, that the flow may distribute inequally on the parallel ducts and that this distribution may change arbitrarily. For this reason the number of parallel ducts was limited to four. The homogeneous distribution of the incoming flow before the muffler was guaranted by inserted gauze screens. These screens also avoided flow separation in the diverging horn between blower and muffler. Each of the four ducts in the muffler has a sine-shaped curvature. The "amplitude" of the sine was choosen in an appropriate relation to the cross-sectional dimensions of the ducts in order to keep the pressure losses small. The attenuation of frequencies above 800 cps is achieved by rockwool behind perforated sheets at the side walls of the ducts, for lower frequencies the attenuation is procured by Helmholtz-resonators in the upper and lower walls of the ducts. Since attenuation with layers of rockwool is greatest for frequencies, where the thickness of the layer equals a quarter wavelength, the curvature of the ducts yields an even frequency response of the attenuation. The Helmholtz-resonators are slit resonators tuned to frequencies about 150 and 300 cps. Fig.3 shows the first element of the muffler with one side wall removed. Fig.4 brings the results of attenuation measurements of the muffler. Above 1 kc the attenuation was greater than the signal-to-noise ratio of the experimental equipment, which determined the limits of these measurements at the dashed line of the graph.

The pressure losses in the muffler and at the several gauze screens are comparable to those of the cooler being about 100 mm water column. The cooler, to be seen on the left hand side of Fig.1, was necessary, since the air leaves the five-stage centrifugal blower with temperatures of about 70 centigrades. The blower is driven by a motor of 60 kW and has a weight rate of flow of about 50 cubic meters per minute against a pressure of 3000 mm water column. For reasons of sound insulation it is installed in a separate room with a sound-proof door to the test room. Variation of flow velocity is achieved by regulation of the slip-ring rotor motor and by a regulating-gate at the inlet of the blower.

§ 2. Test Section of the Duct.

The lateral dimensions of the test section of the duct are 35 times 100 mm. It has a length of 2.40 m. The absorber to be tested is put on one broad side of the duct. The small cross-section was choosen because

a) a stationary flow profile is reached after a short length,
b) turbulence diameters remain small compared to the acoustic wavelength, so scattering of sound by turbulence is avoided,
c) the boundary layer thickness is small compared to the acoustic wavelength, so a constant phase velocity is present over the whole of the cross-sectional area,
d) we are interested mainly in the attenuation of the fundamental mode of the wave in the duct,
e) the acoustic intensity becomes great with the signal generators available.

Fig.5 gives a schematical view of the test section with a rock-wool absorber to be tested. The absorber is enclosed in an air-tight housing. The microphone probe is moved along the duct with the help of a perforated steel band. The steel band runs in two guide grooves and is driven by cam disks at either end of the test section. The band returns in an airtight through below the test section. In order to avoid propagation of structure-

borne sound along the band, it is glued with a rubber tape. The microphone itself is fastened at the steel band with an acoustic low pass filter inserted. This filter consists of a sandwich-like subsequence of brass plates and rubber sheets. This vibration insulation is necessary when microphones of the condensor type are used as described in a following section. By this arrangement of the microphone driving continous registration of the acoustic pressure along the duct is possible with a constant flow resistance due to the insertion of the probe whatever the position of the probe is.

§ 3. Performance of the Wind Tunnel.

The performance of the tunnel was checked with a test section with smooth rigid walls. Measurements with a pitot tube or a hot-wire anemometer were performed at several positions along the test section. The distances of these positions from the duct entrance are indicated on the abscissa of Fig.6. There the variation of the center flow velocity and of the static excess pressure are plotted over the length of the duct for two numbers of revolution of the blower. The maximum available flow velocity is 220 m/sec. The final flow profile and therewith the final velocity in the smooth duct are reached after a distance of about 1.5 meters. In a duct with rough walls stationary values are obtained sooner. Fig.7 shows two profiles of the mean flow velocity and of the associated turbulence levels. The displacement thickness δ^* of 1.9 mm agrees with the theory of turbulent boundary layers. The turbulence level of $6 \cdot 10^{-3}$ on the axis of the duct could yet be improved by insertion of a longer duct section between the last gauze screen and the contraction cone. The cross sectional distribution of the turbulence is in agreement too with the theory. Fig.8 shows the variation of the turbulence level with center flow velocity for several positions along the duct. Small flow velocities were obtained by throttling down the blower. The increase of the turbulence level at these small velocities is caused by pulsating of the excessively throttled blower. The increase

at high flow velocities comes from the gauze screens. These screens do not generate turbulence as long as the Reynolds number related to the diameter of the wires is smaller than 30. The screens used for these measurements had an upper limit of the flow velocity in the test section of about 180 m/sec. In fact the turbulence level is almost independent of flow velocity up to 180 m/sec.

For an estimation of the noise level caused by turbulence during acoustic measurements the turbulence level was analysed with a bandwidth of 10 cps. In the frequency range from 300 to 3000 cps, which is of interest in attenuation measurements, the turbulence velocity amplitude (for 10 cps band width) decreases from $0.4 \cdot 10^{-3}$ to $0.15 \cdot 10^{-3}$ of the mean flow velocity. It is rather independent of the flow velocity. At a flow velocity of 150 m/sec a mean turbulence level of $0.3 \cdot 10^{-3}$ corresponds to a particle velocity of 6 m/sec. In a plane sound wave with the same particle velocity the sound pressure is 250 dyne/cm^2 corresponding to 120 dB relative to $2 \cdot 10^{-4}$ dyne/cm^2. This level can easily be reached with the available loudspeakers. However, for a velocity sensitive probe like the hot wire anemometer there is not enough signal-to-noise ratio left. If a pressure sensitive probe is used, it is to be kept in mind, that with turbulence the velocity and the corresponding pressure detected by the microphone are not related with one another over the characteristic impedance of air but over a factor, which can be smaller by several orders of magnitude. The value of this factor depends on the shape of the microphone and the position of the pick-up on the body of the microphone. (For these conversion factors with an individual pressure probe see Part A of this paper, page 20).

§ 4. Microphone with Small Self-Noise.

A criterion for a good microphone probe appropriate for measurements in flow with high velocities is a small conversion factor of turbulence velocity amplitudes into associate pressure and a small self-noise, that is noise which is generated at the microphone itself. For small conversion factors the pick-up must

be on the side of the probe body, for small self-noise registered by the probe the pick-up must be flush with the wall and must be at a position with a laminar boundary layer. For optimal achievement of these prerequisites a condenser type microphone was developed, a cross section of which is shown in Fig.9. The body of the microphone has the form of a so-called laminar profile. The upstream section is an ellipsoid of revolution. This form is superior over a circular cone. The boundary layer at this body is laminar until the position with largest diameter. The pressure sensitive element is the condenser on the upstream section formed by a 20 μ thick metallized insulating foil and the brass body of the probe, on which the foil is glued along its rim. The signal-to-noise ratio achieved with this microphone for 50 Watts input power at the loudspeakers and a filter bandwidth of 10 cps is plotted in Fig.10 The dashed curves are valid for the probe used in ref.[1] of Part A.

§ 5. First Attenuation Measurements with the New Duct.

As a first absorber a layer of rockwool 7.5 cm thick covered with a perforated steel sheet was measured. In contrast to former measurements with this type of absorber it was now covered with panels not only on its back but also on its sides, so that acoustic radiation and steady flow through the porous material was prohibited.(cf. Fig.5). Fig.11 shows the results of these measurements. There the attenuation in dB per meter is plotted versus frequency with the flow velocity as parameter. The signal, a pure sine wave, propagated in the downstream direction. As in the former measurements with porous absorbers the attenuation decreases almost uniformly over the whole frequency range up to frequencies, where the attenuation for air at rest is limited by the formation of so-called "sound beams". This limitation of the attenuation for high frequencies where the lateral dimensions of the duct become comparable with one half of the wavelength in the duct, is caused by the fact, that there the acoustic energy concentrates on the axis of the

duct and the energy exchange with the wall becomes smaller. For those frequencies the lateral distribution of the acoustic field as described by a transversal wavenumber k_t is the most important factor influencing the attenuation. The influence of flow on the attenuation in this frequency range can be completely described by the change of the transversal wavenumber by the flow as will be discussed later.

Fig.12 shows the results of similar measurements but now the signal propagating in the upstream direction. Here again the principal influence of the flow is based on the change of the acoustic wavelength. Differences of the attenuation as compared with the downstream propagation will become more clear, when the effect of the convective variation of the signal velocities by the flow will be eliminated.

For this elimination of the convective effect we must go back to the definition of the attenuation constant $\alpha = -dN/N$, where $-dN$ is the acoustic power emerging from the duct per unit duct length and N is the power through the cross sectional area S of the duct. For a given acoustic energy density e the value of $-dN$ is given as a function of the admittance G : $-dN = e.f(G)$. We assume G not to be changed by the flow. N for a plane wave is given by $N = eSu_e$, where u_e is the velocity of energy propagation. It equals here to the group velocity u_{gr}. With the approximate assumption of a one-dimensional flow V it follows from the definition of u_{gr} that the group velocity with superimposed flow is $u_{gr,V} = u_{gr,o} + V$. Therefore N with superimposed flow becomes

$$N_V = eS(u_{gr,o}+V) = eSu_{gr,o}(1 + V/u_{gr,o}). \qquad (1)$$

Regardless of a possible change in e (as long as it is constant over the cross sectional area) the attenuation becomes

$$\alpha_V = \frac{\alpha_o}{1+V/u_{gr,o}} \quad . \qquad (2)$$

The attenuation per wavelength α' (the wavelength measured in the duct) then becomes

$$\alpha'_V = \alpha_V \lambda_V = \alpha_V \lambda_o \left(1 + \frac{V}{u_{ph,o}}\right) = \alpha'_o \frac{1 + V/u_{ph,o}}{1 + V/u_{gr,o}} \qquad (3)$$

If α^*_V is defined by the quotient of α'_V divided by the last factor in equ.(3), it follows, that α^*_V should be equal to $\alpha^*_o = \alpha'_o$ if the convective effect would be the only one influencing the attenuation, and if the assumptions made above were exact. But even a violation of the assumptions that the flow be one-dimensional and that the lateral distribution of the acoustic energy density e be unchanged by the flow would not affect the value of the reduction of equ.(3), because this equation shall help to separate the different flow effects. Therefore deviations of α^*_V from α^*_o can be ascribed to variations of the wall admittance L or to influences of the flow profile.

In order to check these relations the wavelength λ_o and the phase velocity $u_{ph,o}$ were measured in the duct with air at rest and are plotted in Fig.13. From a smooth curve through the measured values of $u_{ph,o}$ the group velocity $u_{gr,o}$ was calculated according to

$$u_{gr} = \frac{u_{ph}}{1 - \frac{f}{u_{ph}} \frac{du_{ph}}{df}} \quad . \qquad (4)$$

From smooth curves through the measured values of the figures 11 and 12 then α^*_V was calculated. This value is represented in Fig.14 for the downstream propagation of the signal. One sees clearly a systematic decrease of the corrected value of the attenuation for low frequencies up to 2.5 kc, where according to Fig.11 the acoustic beam formation becomes important. The causes of this decrease shall be studied in

further measurements. According to the results in Part A of this paper they must be caused however by nonlinearity of the absorber and by the influences of the flow profile. It is worthwhile to note, that the deviations of α_V^* from α_o^* are enhanced by the last factor of equ.(3). This factor decreases from 1.07 at 0.3 kc to 1.00 at 2 kc for V = 60 m/sec and from 1.16 at 0.5 kc to 1.00 at 2 kc for V = 180 m/sec. Above 2 kc it is unity. Fig.14 shows also, that for frequencies, where the cross dimensions of the duct become comparable to one half of a wavelength, most of the influence of the flow on the attenuation is taken into account by considering attenuation values at constant wavelengths. This result indicates, that by the convective change of the longitudinal wavenumber k_l also the lateral wavenumber k_t is changed.

Fig.15 shows α_V^* for upstream propagation of the signal. Here the deviations for low frequencies are relatively small, whereas they are great for high frequencies. By application of the results of Part A of this paper it must be expected, that for upstream propagation the influence of the flow profile becomes prevailing, especially at high frequencies. For this direction of propagation the factor between α_V^* and α_V' increases from 0.9 at 0.3 kc to 1.0 at 2 kc for V = -60 m/sec and from 0.4 at 0.3 kc to 1.0 at 2 kc for V = -180 m/sec.

In most practical applications of absorbers, these are exposed to broad-band noise instead to pure tones. The nonlinearity of the absorber under the influence of the flow could lead to the expectation, that the attenuation constant for noise would differ from that for pure tones. Therefore attenuation measurements were performed with the absorber of Fig.5 with third-octave noise as signal. These measurements were possible because of the great signal-to-noise ratios available. The results are plotted in Figures 16 and 17 for downstream and upstream propagation resp. Comparison with the Figures 11 and 10 shows, that the attenuation remains nearly the same. Only for upstream propagation and high frequencies some differences are indicated.

These measurements show, that with the new duct investigations can be performed about the behaviour of absorbers in the presence of a flow much alike as in exhaust mufflers for jet engines. These measurements will be continued.

Fig.1 Wind tunnel section from blower to entrance into measuring path.

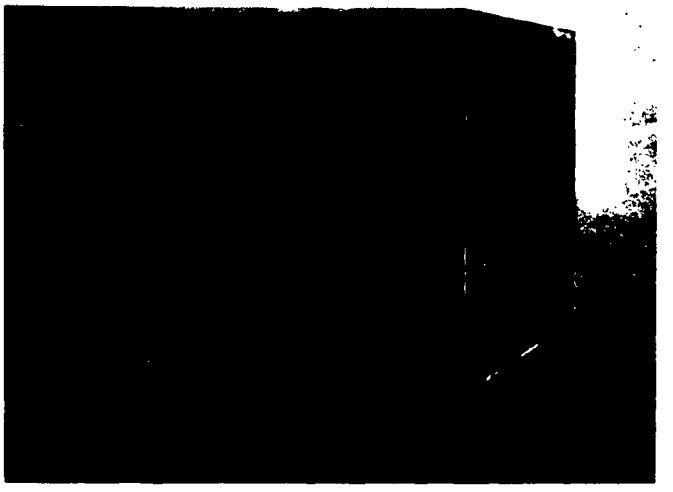

Fig.3 Element of the muffler with one side wall removed.

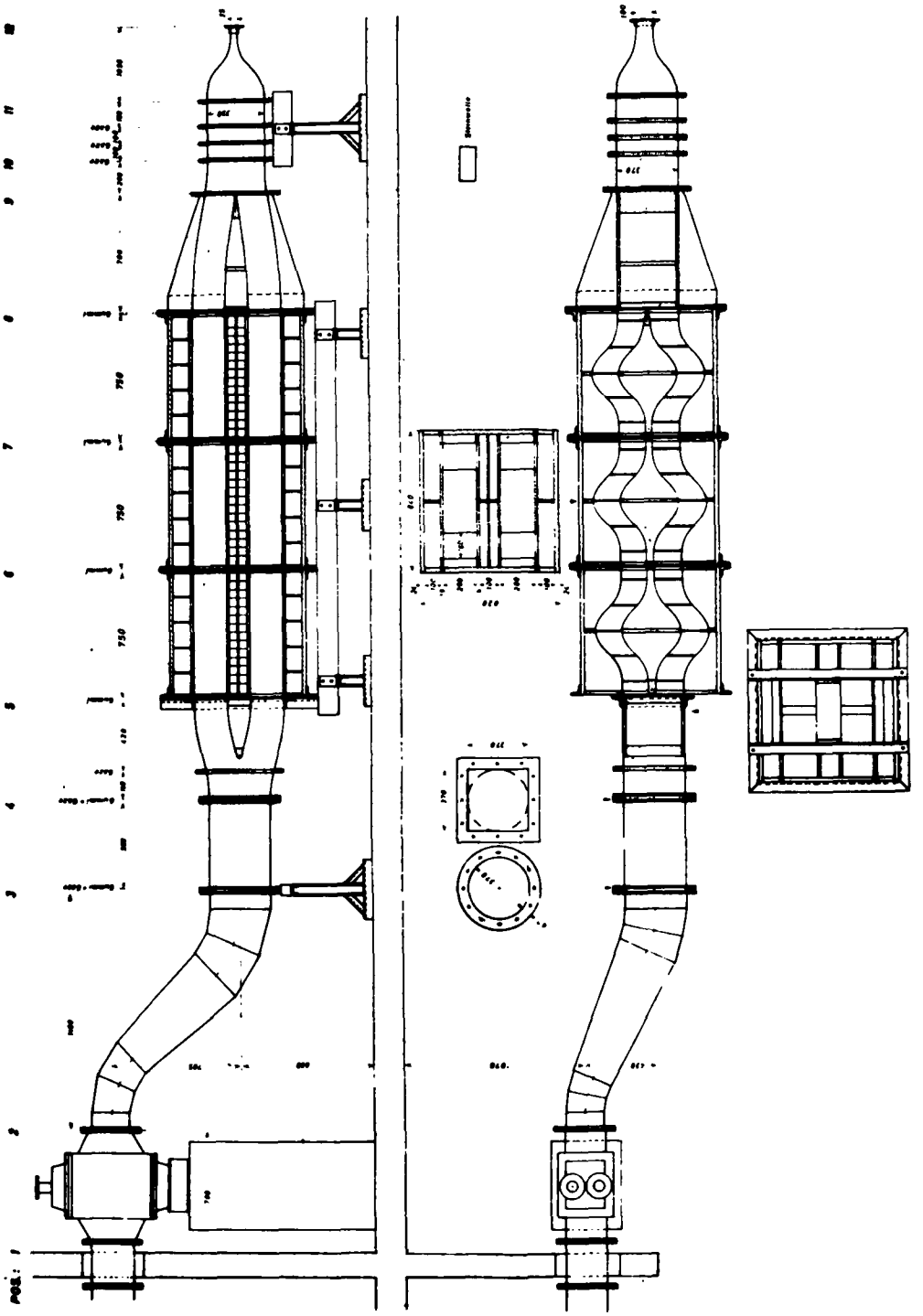

Fig. 2 Cross sections of the muffler.

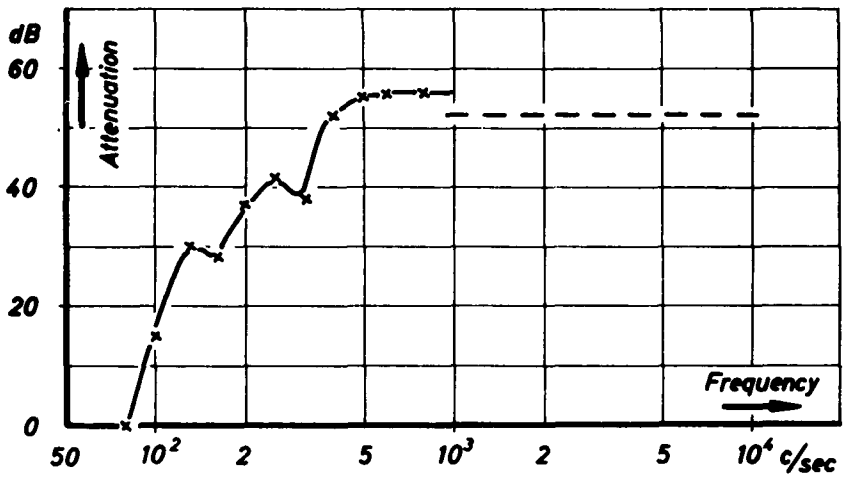

Fig. 4 Attenuation of air-borne sound effected by the attenuator in the new duct.

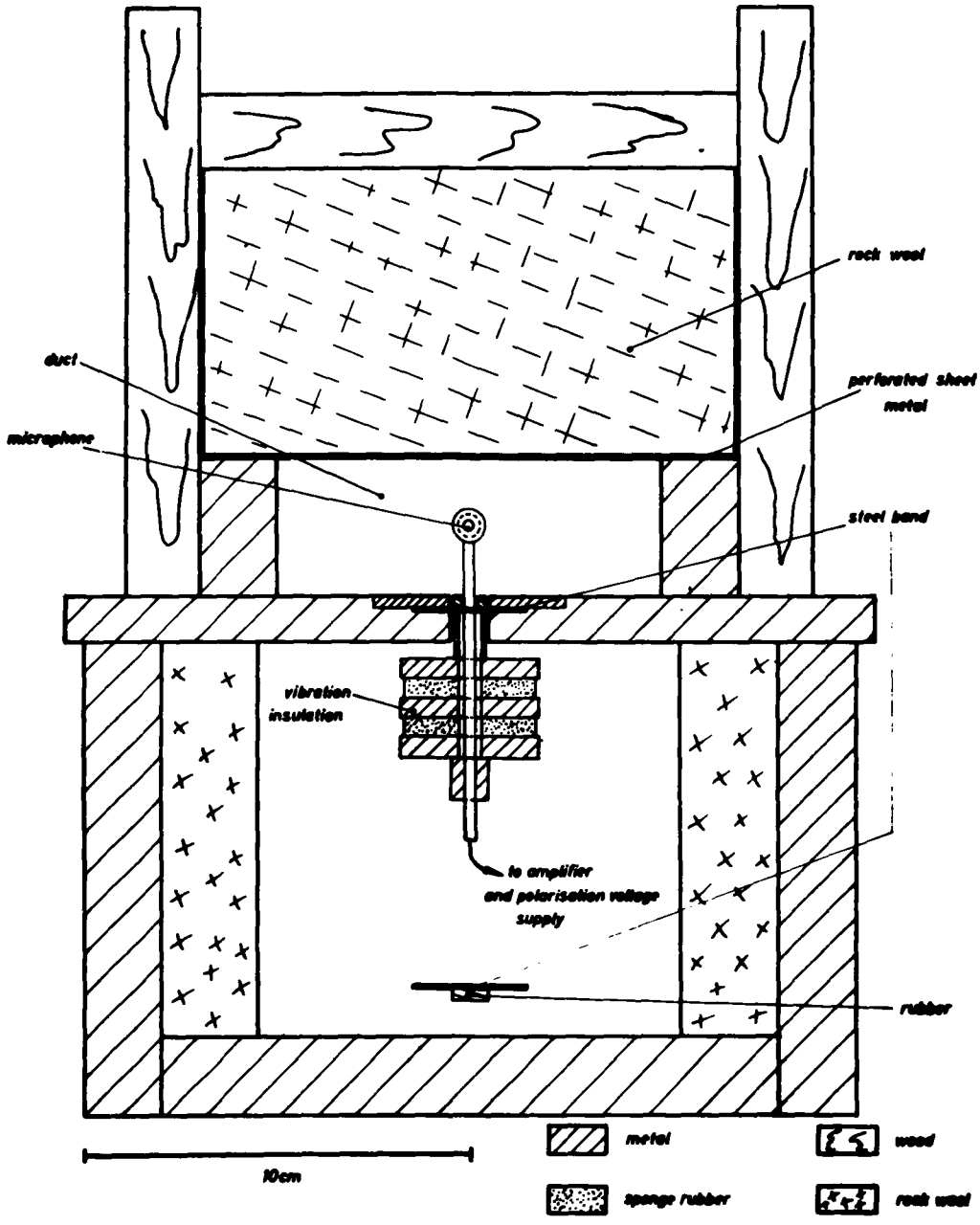

Fig.5 Cross sectional view of the test section with a rockwool absorber under test.

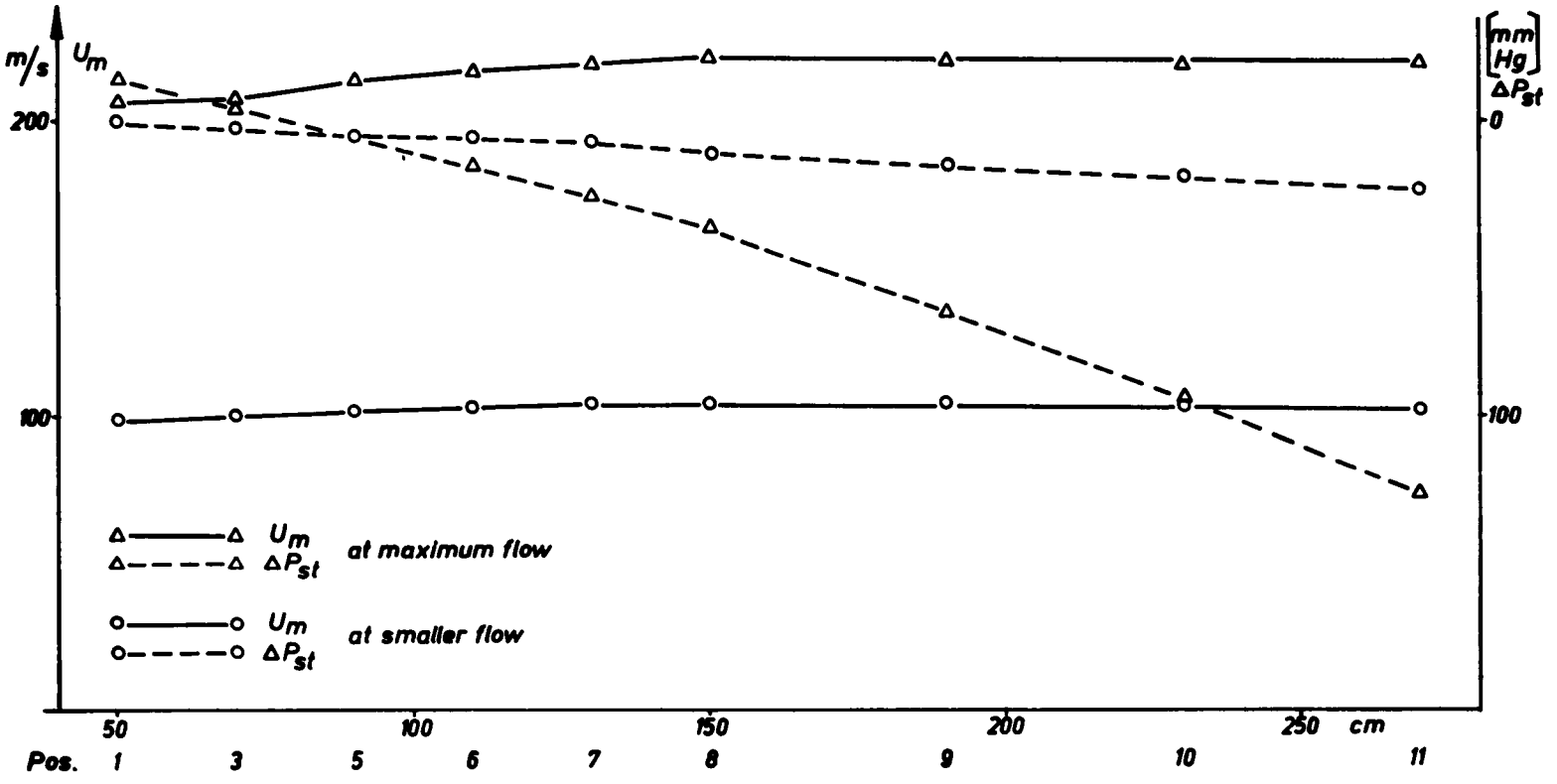

Fig. 6 Variation of velocity and static pressure along channel axis.

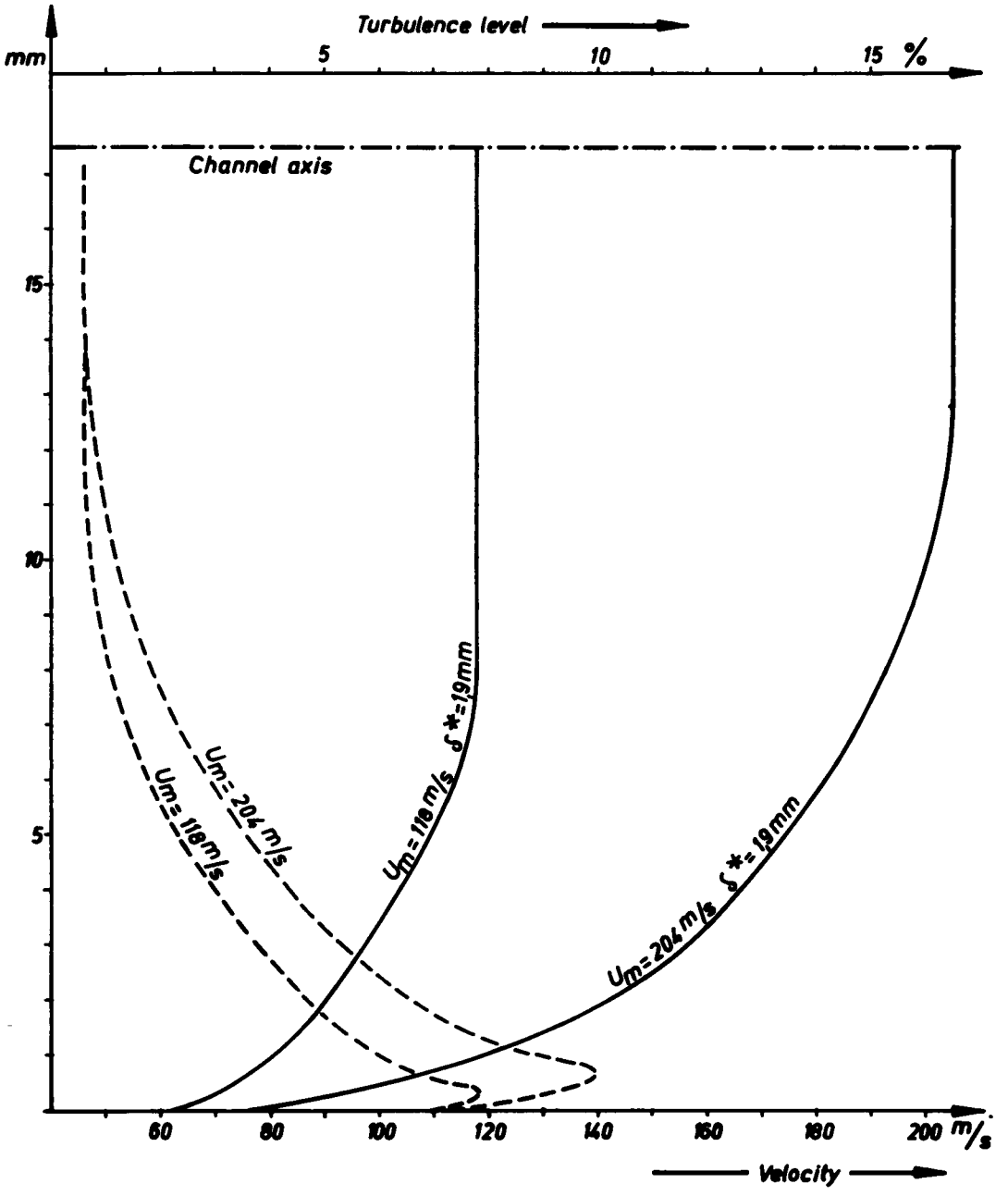

Fig. 7 Velocity and turbulence profiles along vertical center line at position 1 at two center velocities.

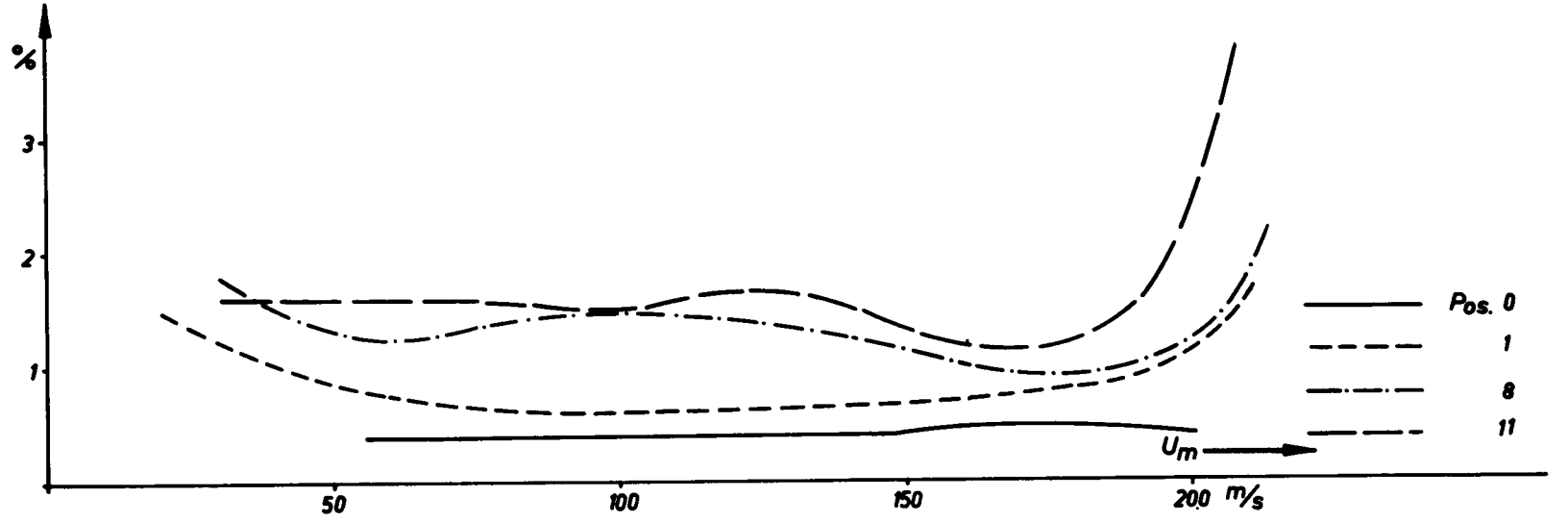

Fig. 8 Variation of turbulence level with center velocity at several positions.

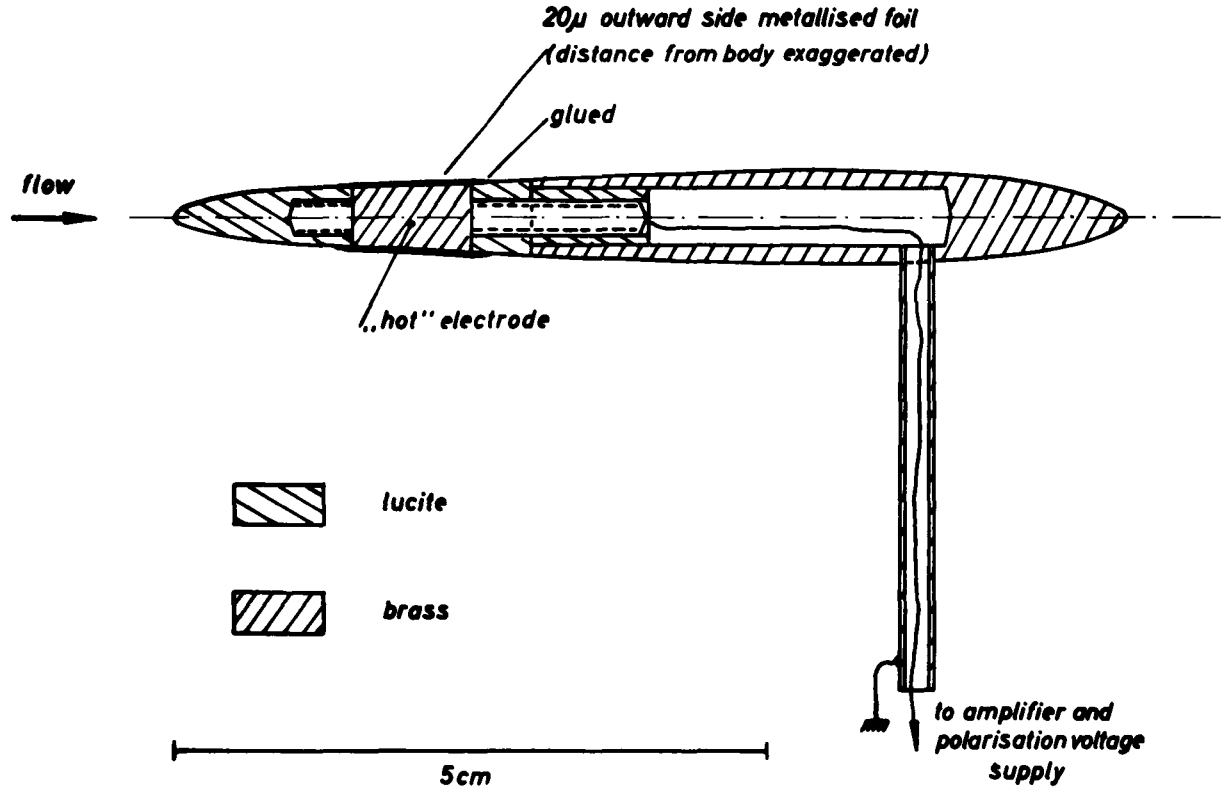

Fig.9 Cross sectional view of the probe microphone.

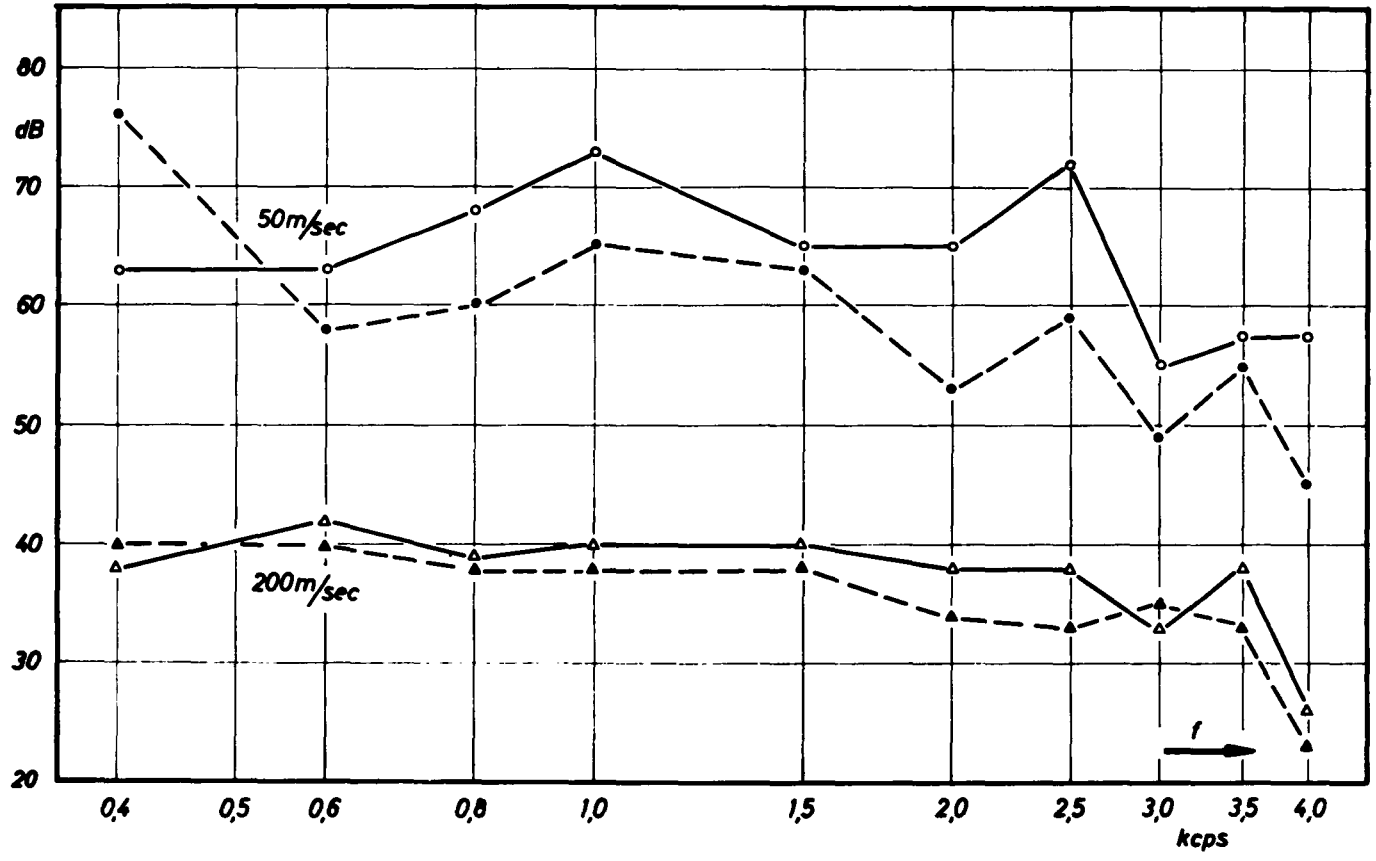

Fig.10 Signal-to-noise ratio obtained with the microphone from Fig.9 for 50 Watts loudspeaker input. Dashed curves are valid for the probe used in ref.[1] of part A.

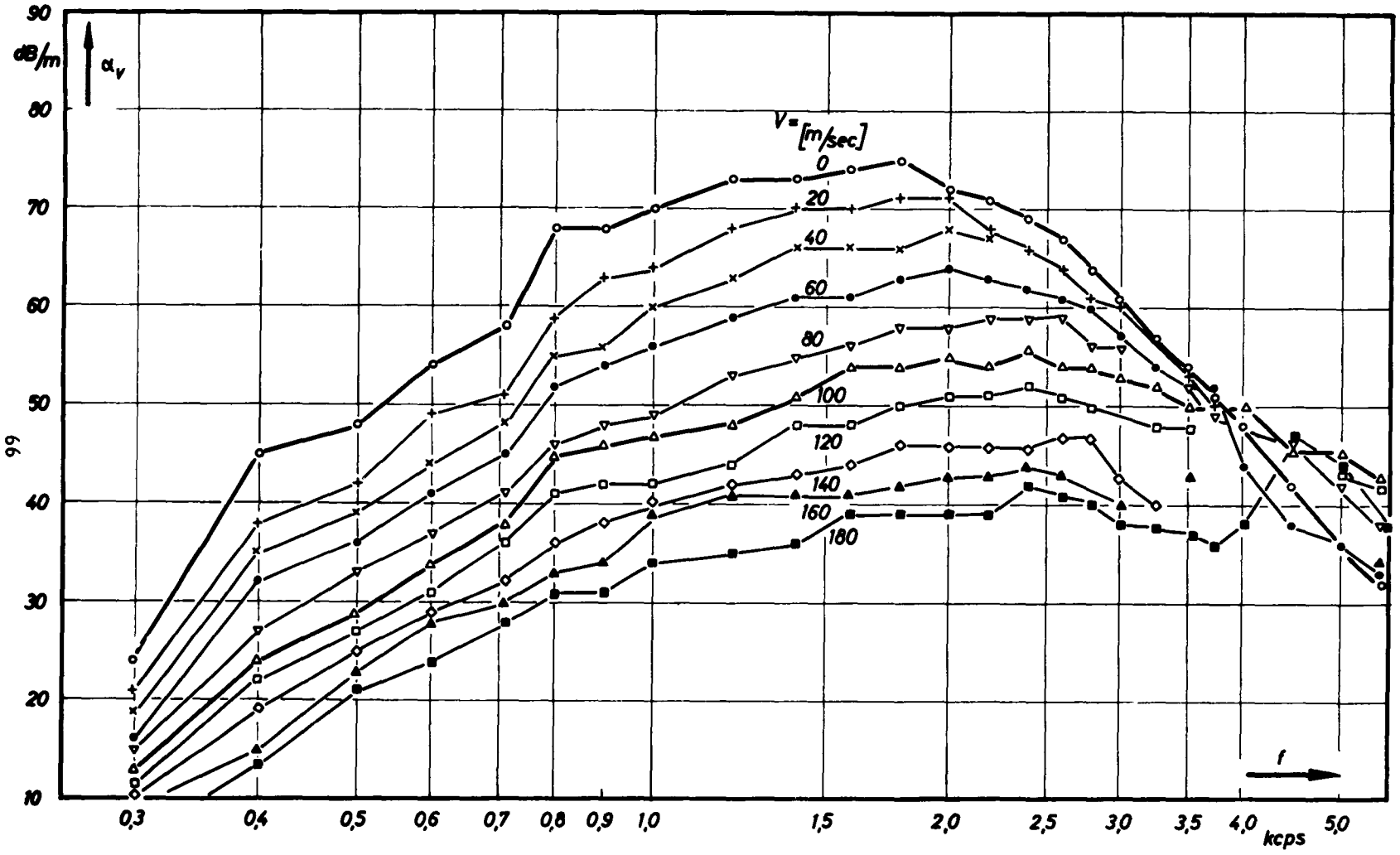

Fig. 11 Attenuation of a porous absorber (Fig.5) for downstream propagation with pure tones as signal.

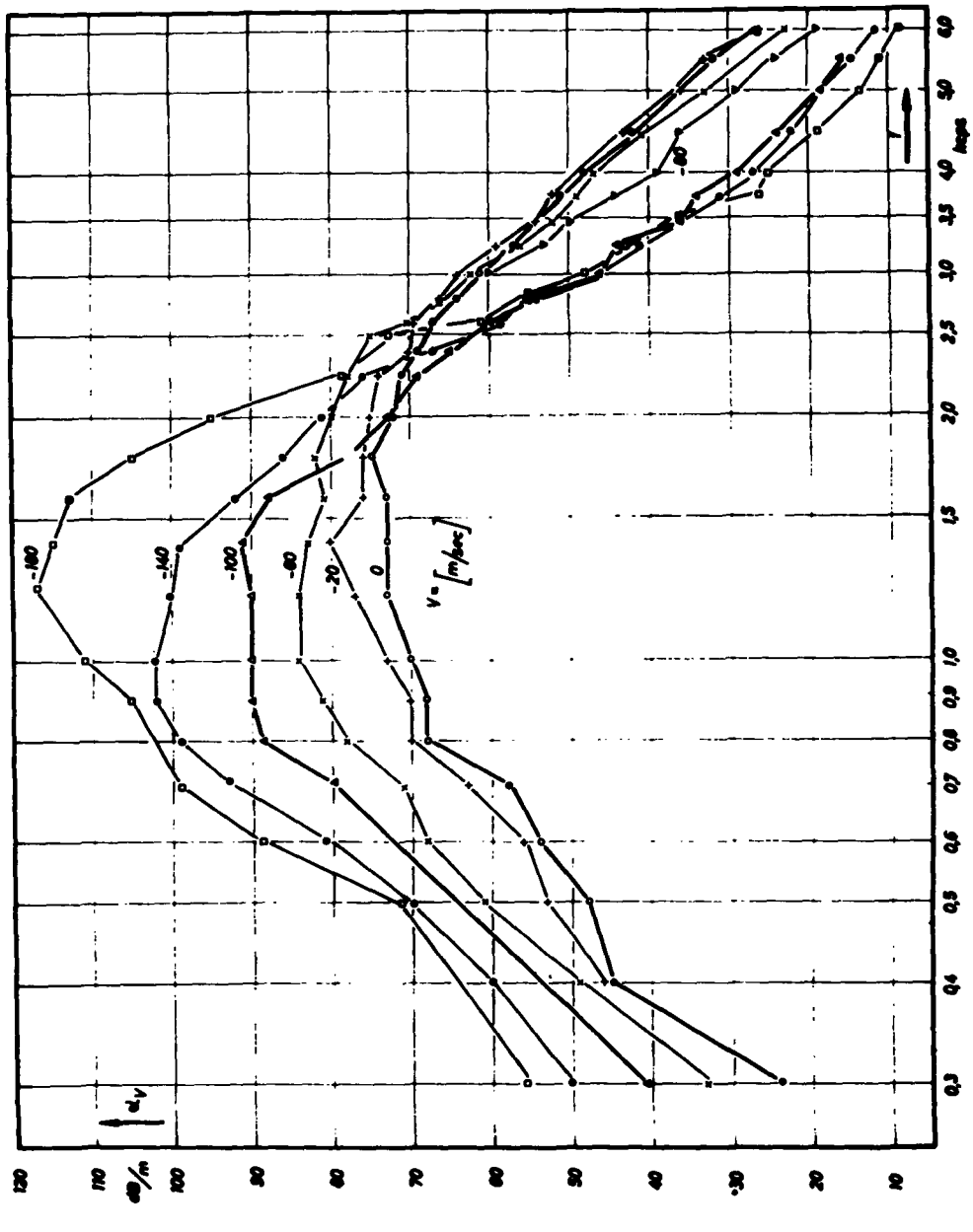

s in Fig.11 but for upstream propagation.

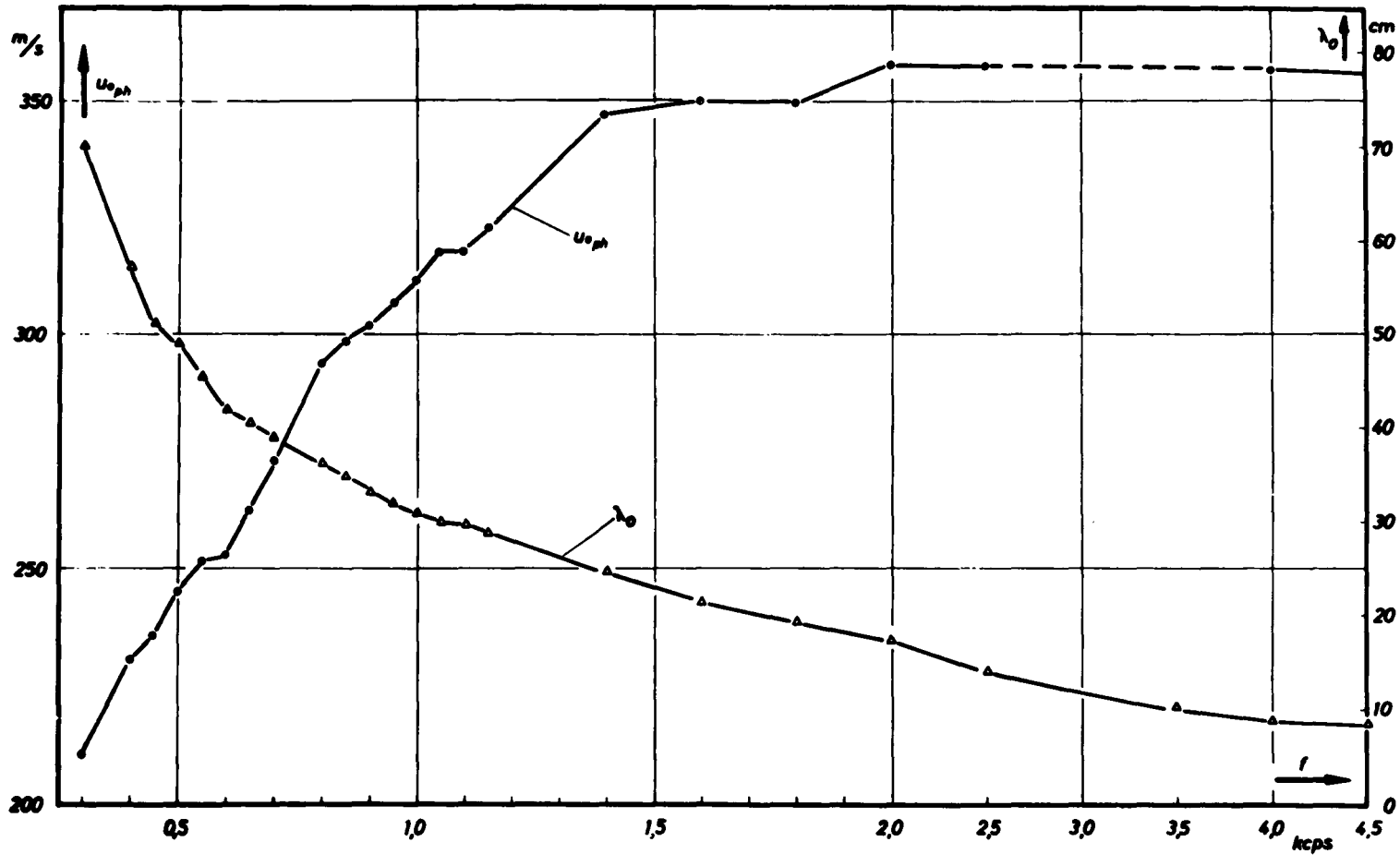

Fig. 13 Wavelength and phase velocity in the duct of fig.5.

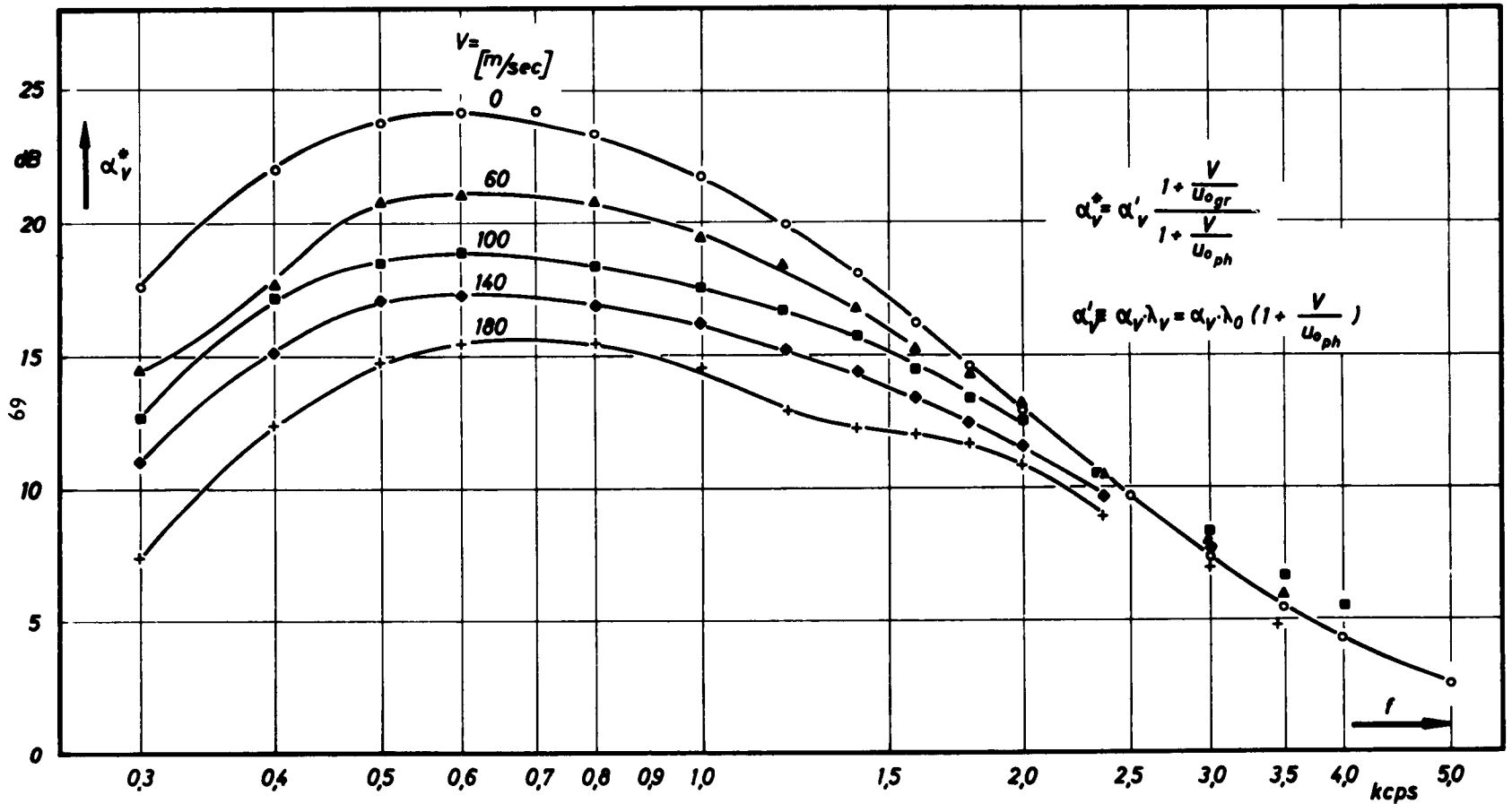

Fig. 14 Reduction of the attenuation of Fig.11 for elimination of the signal convection.

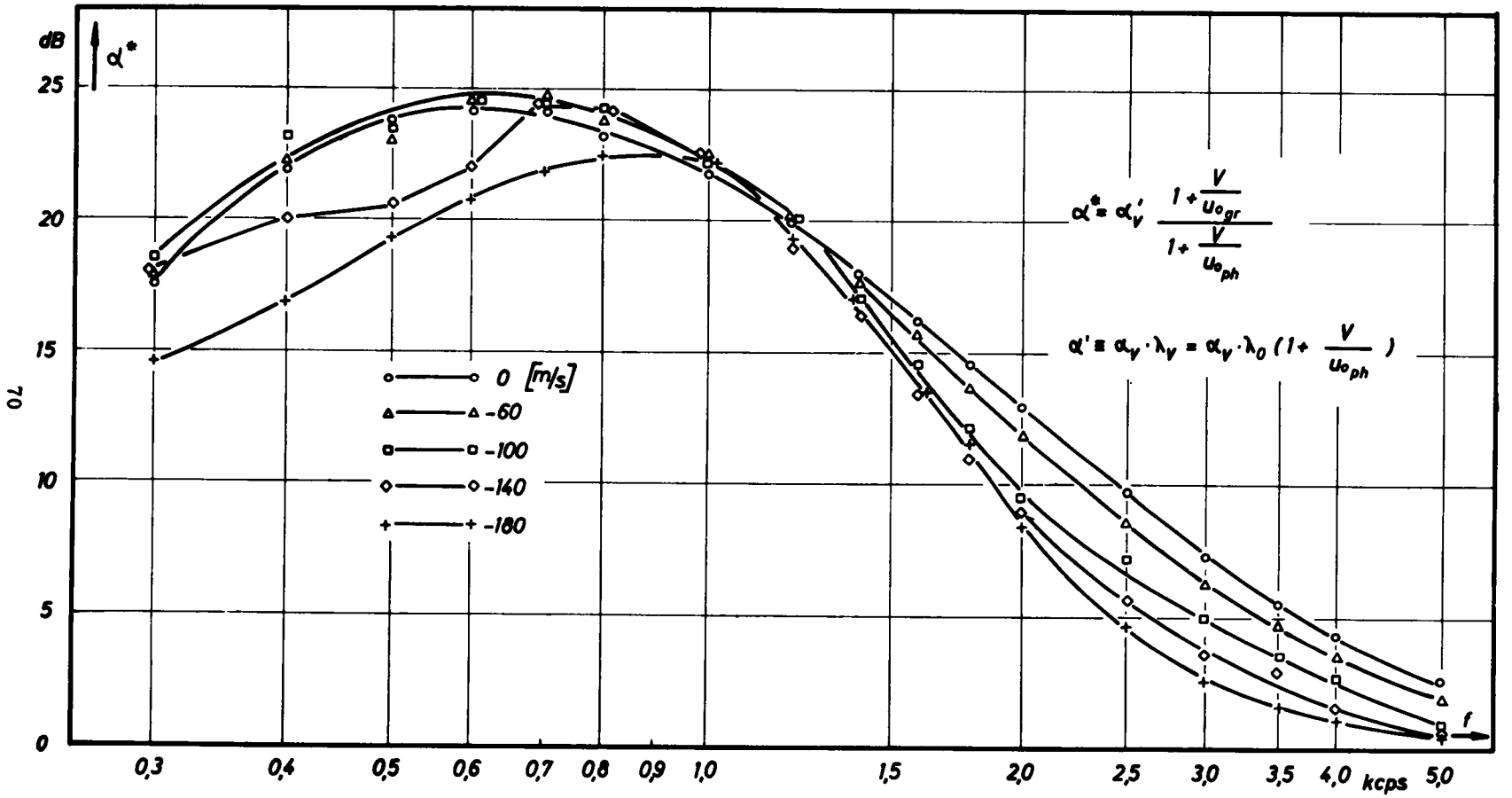

Fig. 15 Reduction of the attenuation of Fig.12 for elimination of the signal convection.

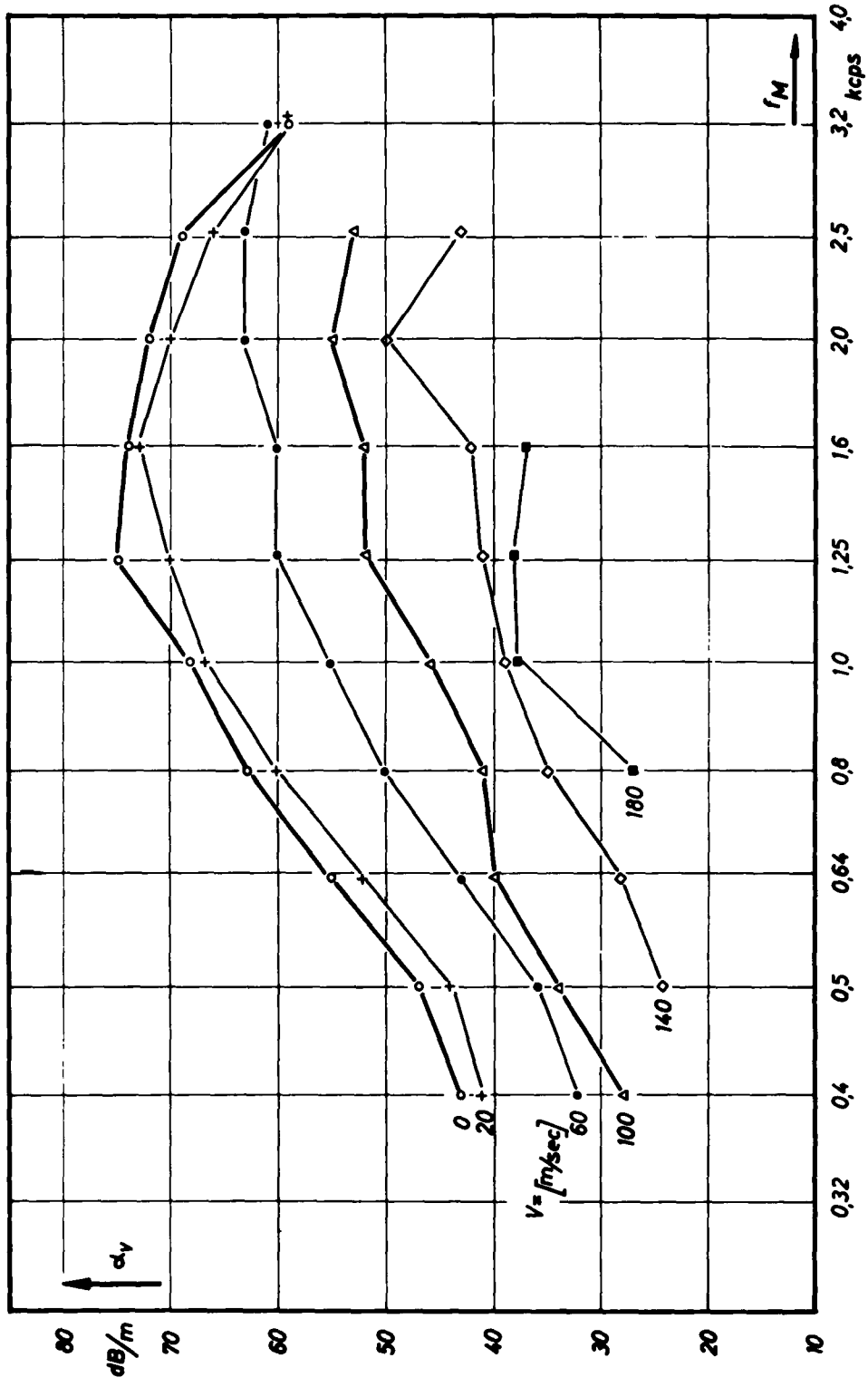

Fig. 16 Attenuation for third-octave noise propagating downstream.

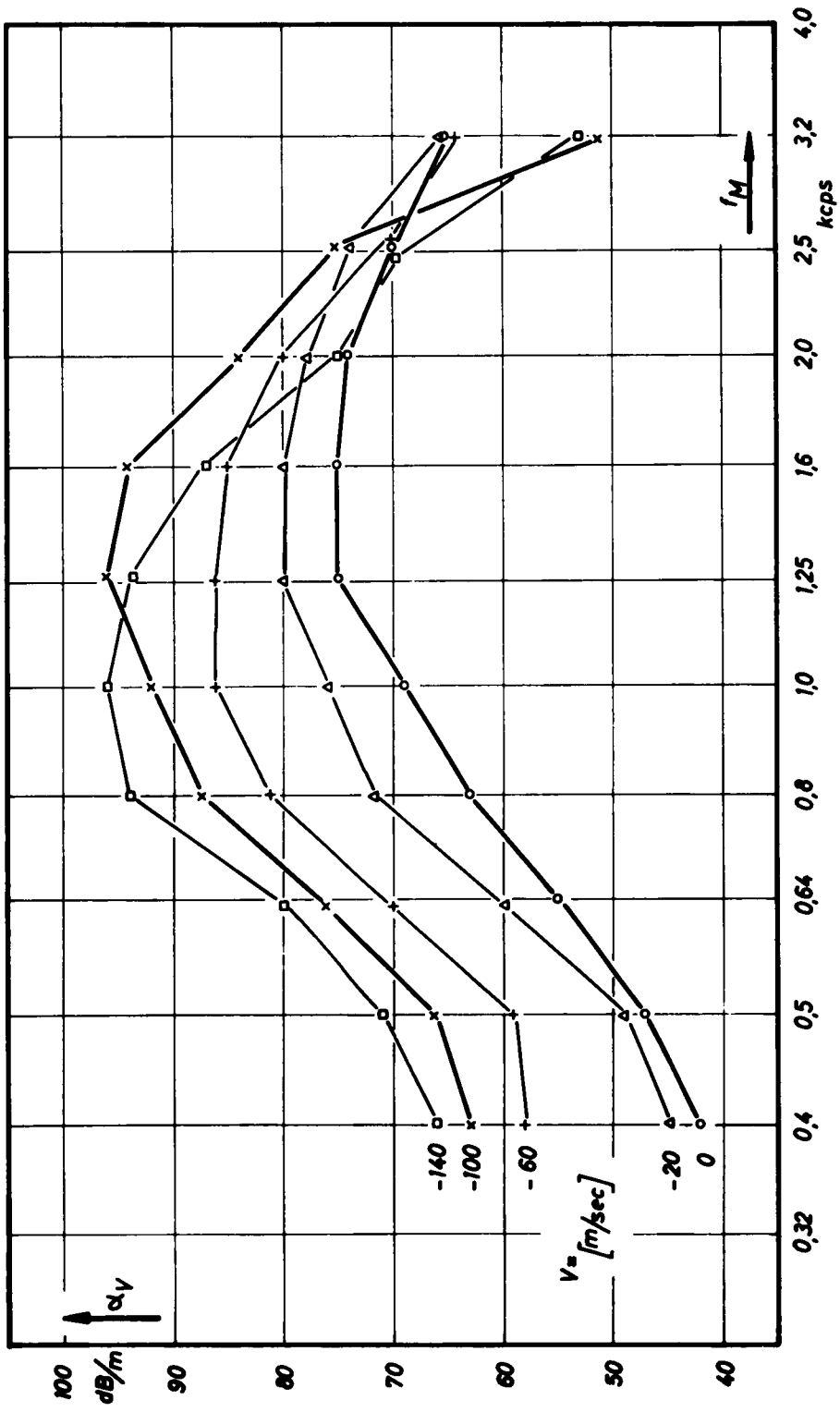

Fig. 17 Attenuation for third-octave noise propagating upstream.

Aerospace Medical Division, 6570th Aerospace Medical Research Laboratories, Wright-Patterson AFB, Ohio Rpt No. AMRL-TDR-62-140 (II). RESEARCH ON SOUND PROPAGATION IN SOUND-ABSORBENT DUCTS WITH SUPERIMPOSED AIR STREAMS (II). Final Rpt, Dec. 62, ix + 72 pp. incl. illus., 4 refs.
Unclassified Report

This report, Volume II, shows that the attenuation of sound in absorbing ducts with superimposed flow is dependent in a high degree on the direction of the flow and its velocity. The change of attenuation is caused by a convective variation of the acoustic wavelength, by a nonlinear variation of the characteristic constants of the absorber, and by a deformation of the wave fronts

(over)

in the profile of the mean flow. These changes can be calculated and are in good agreement with the experimental results. In a duct coated with undamped Helmholtz resonators the mechanism of sound amplification is based on the interaction between the sound wave and the turbulence. The conversion of kinetic flow energy into acoustic energy is performed by synchronization of turbulence. For appropriate values for flow velocity and signal frequency a long-range stable wave of pseudo-sound takes place. Sound and pseudo-sound interact with one another at the necks of the resonators.

UNCLASSIFIED

1. Attenuation (wave propagation)
2. Sound transmission (sound and acoustics)
3. Acoustics (sound and acoustics)

I. AFSC Project 7231, Task 723104
II. Biomedical Laboratory
III. Contract AF 61(052)-112
IV. Göttingen University, Göttingen, Germany
V. Mechel, F. Schilz, W.
VI. In ASTIA collection
VII. Avail fr OTS $2.25

UNCLASSIFIED

Aerospace Medical Division, 6570th Aerospace Medical Research Laboratories, Wright-Patterson AFB, Ohio Rpt No. AMRL-TDR-62-140 (II). RESEARCH ON SOUND PROPAGATION IN SOUND-ABSORBENT DUCTS WITH SUPERIMPOSED AIR STREAMS (II). Final Rpt, Dec. 62, ix + 72 pp. incl. illus., 4 refs.
Unclassified Report

This report, Volume II, shows that the attenuation of sound in absorbing ducts with superimposed flow is dependent in a high degree on the direction of the flow and its velocity. The change of attenuation is caused by a convective variation of the acoustic wavelength, by a nonlinear variation of the characteristic constants of the absorber, and by a deformation of the wave fronts

(over)

in the profile of the mean flow. These changes can be calculated and are in good agreement with the experimental results. In a duct coated with undamped Helmholtz resonators the mechanism of sound amplification is based on the interaction between the sound wave and the turbulence. The conversion of kinetic flow energy into acoustic energy is performed by synchronization of turbulence. For appropriate values for flow velocity and signal frequency a long-range stable wave of pseudo-sound takes place. Sound and pseudo-sound interact with one another at the necks of the resonators.

UNCLASSIFIED

1. Attenuation (wave propagation)
2. Sound transmission (sound and acoustics)
3. Acoustics (sound and acoustics)

I. AFSC Project 7231, Task 723104
II. Biomedical Laboratory
III. Contract AF 61(052)-112
IV. Göttingen University, Göttingen, Germany
V. Mechel, F. Schilz, W.
VI. In ASTIA collection
VII. Avail fr OTS $2.25

UNCLASSIFIED